Supporting Information for

Self-assembly and guest-induced disassembly of triply interlocked [2]catenanes

Ying-Ying Zhang,*[a] Feng-Yi Qiu,[b] Hua-Tian Shi[b] and Weibin Yu*[b]

[a.] *Center for Advanced Materials Research, Henan Key Laboratory of Functional Salt Materials, Zhongyuan University of Technology, Zhengzhou 450007, P. R. China. E-mail: 6477@zut.edu.cn*

[b.] *Analysis and Testing Central Facility, Engineering Research Institute, Anhui University of Technology, Maanshan 243002, P. R. China. E-mail: yuweibin@ahut.edu.cn*

Table of contents

1. Experimental Procedures

1.1 General

All reagents and solvents were purchased from commercial sources and used as supplied unless otherwise mentioned. The starting material $[Cp^*RhCl_2]_2$ (Cp^*= η5-pentamethylcyclopentadienyl) was prepared by the literature method.[1] NMR spectra were recorded on Bruker AVANCE I 400 at room temperature and referenced to the residual protonated solvent for NMR spectra. Proton chemical shift $\delta_H = 5.32$ (CD_2Cl_2), δ_H = 3.31 (CD_3OD) are reported relative to the solvent residual peak. Elemental analyses were performed on an Elementar Vario EL cube analyzer. IR spectra of the solid samples (KBr tablets) in the range 400-4000 cm^{-1} were recorded on a Nicolet AVATAR-360IR spectrometer. UV spectra were recorded on a UV-VIS-NIR Spectrophotometer UV-3600 purchased from SHIMADZU in the range 185-3300 nm in solution. Fluorescent spectra were recorded on a fluorospectrophotometer (FLS 980) purchased from EDINBURGH INSTRUMENTS. ESI-TOF-MS spectra were recorded on a Micro TOF II mass spectrometer and a Waters Synapt G2 mass spectrometer using electrospray ionization. Thermogravimetric analyse (TGA) was recorded by the Netzsch STA 449C thermal analyzer at a heating rate of 10 °C·min^{-1} in air.

1.2 Syntheses of complexes 1, 2 and 3

1.2.1 Synthesis of 1

Treatment of $[Cp^*RhCl_2]_2$ (37.2 mg, 0.06 mmol) with AgOTf (61.2 mg, 0.24 mmol) was in methanol (20 ml) at room temperature, and kept it stirring in the dark overnight. After filtrated, 5,8-dihydroxy-1,4-naphthoquinone (H_2dntq) (11.4 mg, 0.06 mmol) and NaOH (4.0 mg, 0.1 mmol) were added to the filtrate, and vigorously stirred at room temperature for 24 hours to produce a dark green solution. And then, organic ligand tpeb (15.3 mg, 0.04 mmol) was added into the reactive solution. After purified by recrystallization from methanol/diethyl ether, the brown product was obtained. Characterization data for **1** follow: 53 mg, yield 73%. ^{1}H NMR (400 MHz, CD_2Cl_2, ppm): δ = 8.34 (dd, J = 4.0 Hz, 24H, tpeb), 7.78 (s, 12H, tpeb), 7.57 (dd, J = 4.0 Hz, 24H, tpeb), 7.18 (s, 24H, dntq), 1.57 (s, 180H, Cp*). Elemental analysis calcd (%) for chemical formula: $C_{300}H_{264}F_{36}N_{12}O_{60}Rh_{12}S_{12}$: C, 49.35; H, 3.64; N, 2.30; S, 5.27; Found: C, 49.32; H, 3.61; N, 2.26; S, 5.25. ESI-TOF-MS: $[[(C_{10}H_{15}Rh)_{12}(C_{10}H_4O_4)_6(C_{27}H_{15}N_3)_4](F_3CSO_3)_9]^{3+}$ = 2284.48 (calcd : 2284.47).

1.2.2 Synthesis of 2

Treatment of $[Cp^*RhCl_2]_2$ (37.2 mg, 0.06 mmol) with AgOTf (61.2 mg, 0.24 mmol) was in methanol (20 ml) at room temperature, and kept it stirring in the dark overnight. After filtrated, quinizarin (H_2qz) (14.4 mg, 0.06 mmol) and NaOH (4.0 mg, 0.1 mmol) were added to the filtrate, and vigorously stirred at room temperature for 24 hours to produce a dark green solution. And then, tpeb (15.3 mg, 0.04 mmol) was added into the reactive solution. After purified by recrystallization from methanol/diethyl ether, the brown product was obtained. Characterization data for **2** follow: 53.2 mg, yield 70%. ^{1}H NMR (400 MHz, CD_2Cl_2, ppm): δ = 8.44 (m, 24H, tpeb), 7.76 (m, 12H, tpeb), 7.56 (m, 24H, tpeb), 8.66 (m, 12H, qz), 7.98 (m, 12H, qz), 7.28 (dd, *J1* = 4.0 Hz, *J2* = 8.0 Hz, 12H, qz), 1.67 (t, *J* =4.0 Hz, 180H, Cp*). Elemental analysis calcd (%) for chemical formula: $C_{324}H_{276}F_{36}N_{12}O_{60}Rh_{12}S_{12}$: C, 51.20; H, 3.66; N, 2.21; S, 5.06; Found: C, 51.16; H, 3.63; N, 2.17; S, 5.02. ESI-TOF-MS: $[(C_{10}H_{15}Rh)_{12}(C_{14}H_6O_4)_6(C_{27}H_{15}N_3)_4](F_3CSO_3)_9]^{3+}$ = 2384.50 (calcd : 2284.50).

1.2.3 Synthesis of 3

Treatment of $[Cp^*RhCl_2]_2$ (37.2 mg, 0.06 mmol) with AgOTf (61.2 mg, 0.24 mmol) was in methanol (20 ml) at room temperature, and kept it stirring in the dark overnight. After filtrated, 6,11-dihydroxy-5,12-naphthacenedione (H_2dntd) (17.4 mg, 0.06 mmol) and NaOH (4.0 mg, 0.1 mmol) were added to the filtrate, and vigorously stirred at room temperature for 24 hours to produce a dark green solution. And then, tpeb (15.3 mg, 0.04 mmol) was added into the reactive solution. After purified by recrystallization from methanol/diethyl ether, the brown product was obtained. Characterization data for **3** follow: 60 mg, yield 76%. ^{1}H NMR (400 MHz, CD_2Cl_2, ppm): δ = 8.72 (dd, *J1* = 4.0 Hz, *J2* = 8.0 Hz, 12H, tpeb), 8.46 (dd, *J* = 4.0 Hz, 12H, tpeb), 7.64 (s, 6H, tpeb), 7.97 (dd, *J1* = 4.0 Hz, *J2* = 8.0 Hz, 12H, dntd), 7.48 (dd, *J1* = 4.0 Hz, *J2* = 8.0 Hz, 12H, dntd), 1.72 (s, 90H, Cp*). Elemental analysis calcd (%) for chemical formula: $C_{174}H_{144}F_{18}N_6O_{30}Rh_6S_6$: C, 52.90; H, 3.67; N, 2.13; S, 4.87; Found: C, 52.87; H, 3.64; N, 2.11; S, 4.84. ESI-TOF-MS: $[[(C_{10}H_{15}Rh)_6(C_{14}H_6O_4)_3(C_{27}H_{15}N_3)_2](F_3CSO_3)_3]^{3+}$ = 1167.79 (calcd : 1167.79).

1.3 X-ray crystal structure analysis

Single crystals of **1** and **2** suitable for X-ray diffraction analysis were obtained at room temperature. Crystallographic data for complexes **1** and **2** were collected at 173 K with

a Bruker D8 Venture microfocus X-ray source system. The structures were solved by direct methods, and refined on F^2 by a full-matrix least-squares method. In the data, the disordered solvent molecules that could not be adequately restrained were removed using the SQUEEZE routine. CCDC 2021986 (**1**) and 2021987 (**2**) contain the supplementary crystallographic data for this paper. These data are provided free of charge by The Cambridge Crystallographic Data Centre.

Single black block-shaped crystals of **1** were used as supplied. A suitable crystal with dimensions 0.36 x 0.31 x 0.28 mm^3 was selected and mounted on a Bruker APEX-II CCD diffractometer. The crystal was kept at a steady T = 173(2) K during data collection. The structure was solved with the SHELXT 2018/2[2a] solution program using iterative methods and by using Olex2 1.5-dev[3] as the graphical interface. The model was refined with SHELXT 2018/3[2b] using full matrix least squares minimisation on F^2.

A solvent mask was calculated and 897 electrons were found in a volume of 3052 A^3 in **1** void per unit cell. This is consistent with the presence of 2[C1F3O3S], 6[C2H3N] and 4[C4H10O] per Formula Unit which account for 892 electrons per unit cell. The decision to mask two triflate counter ions was not taken lightly, but all other chemical evidence as well as the requirement of the charge balance leave no other conclusion: two triflates are hiding in the solvent sphere. The full, un-masked hkl is embedded in the CIF.

2. Supplementary Figures

2.1 NMR spectra of complexes 1-3

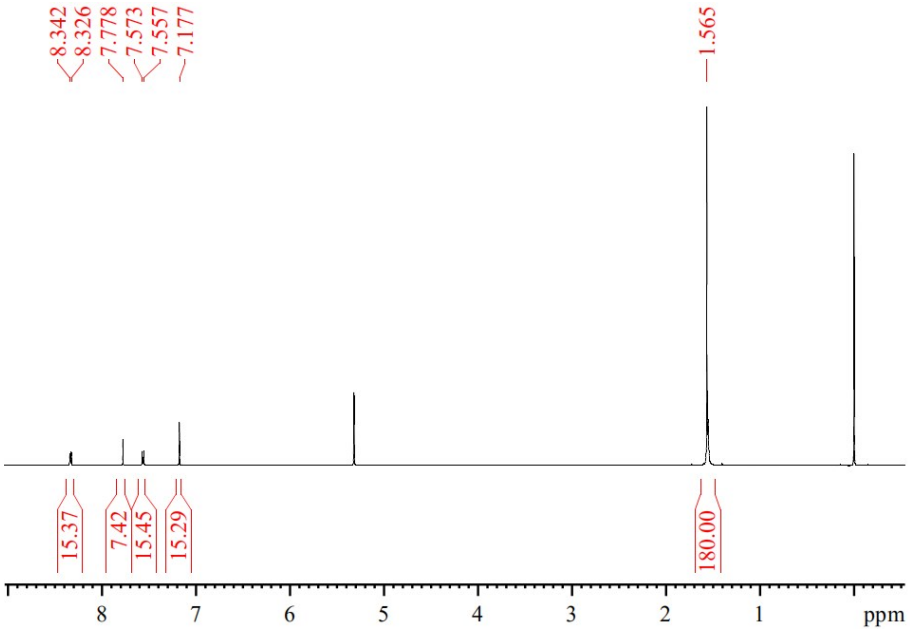

Figure S1. ^{1}H NMR spectrum of **1**.

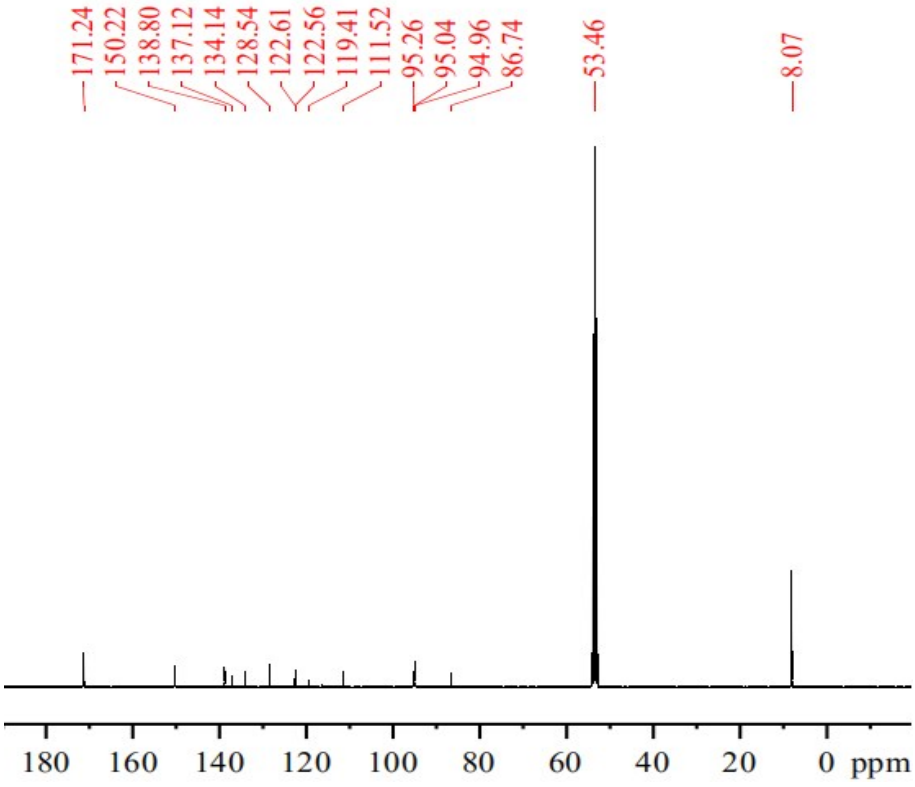

Figure S2. ^{13}C NMR spectrum of **1**.

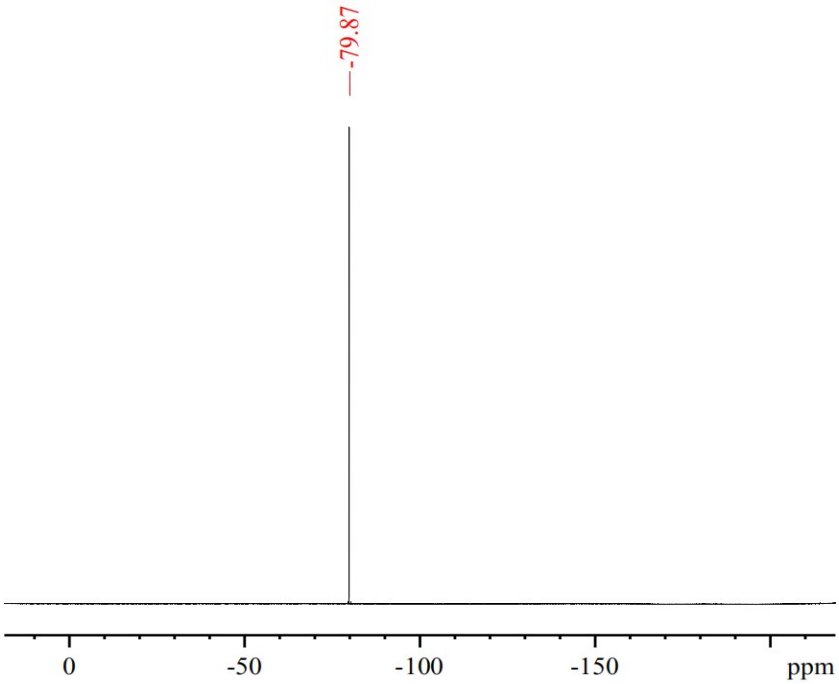

Figure S3. ^{19}F NMR spectrum of **1**.

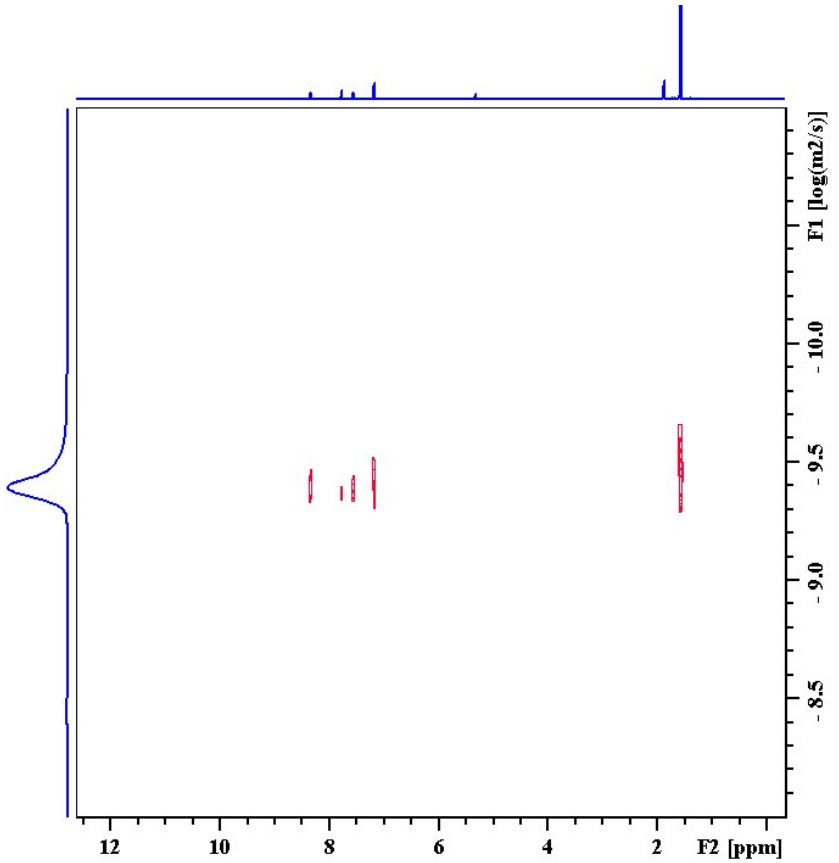

Figure S4. ^{1}H-^{1}H DOSY NMR spectrum of **1**.

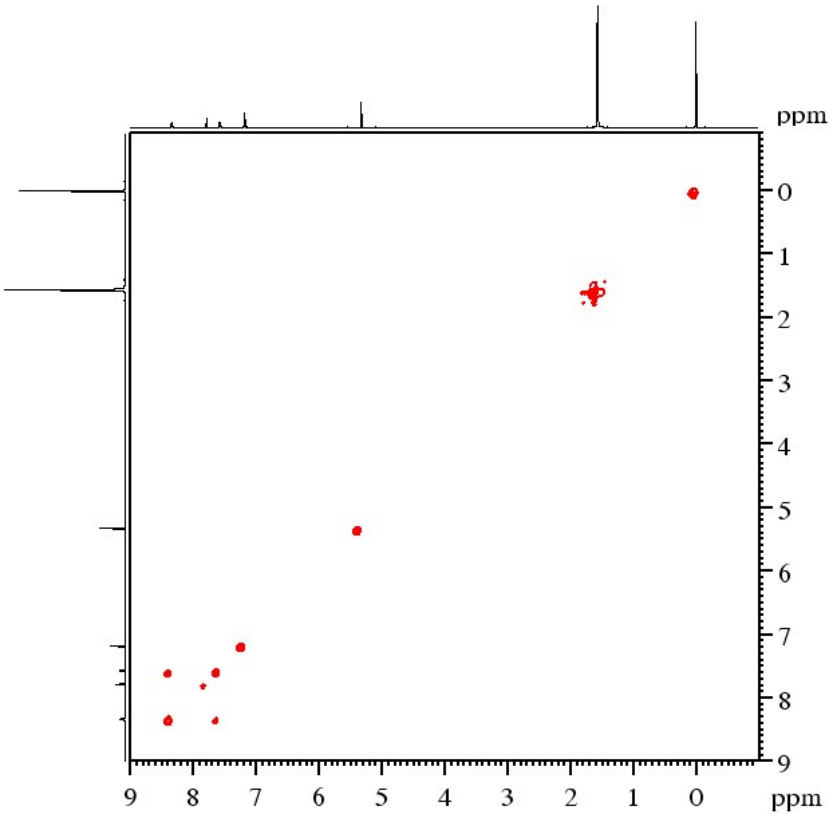

Figure S5. ^{1}H-^{1}H COSY NMR spectrum of **1**.

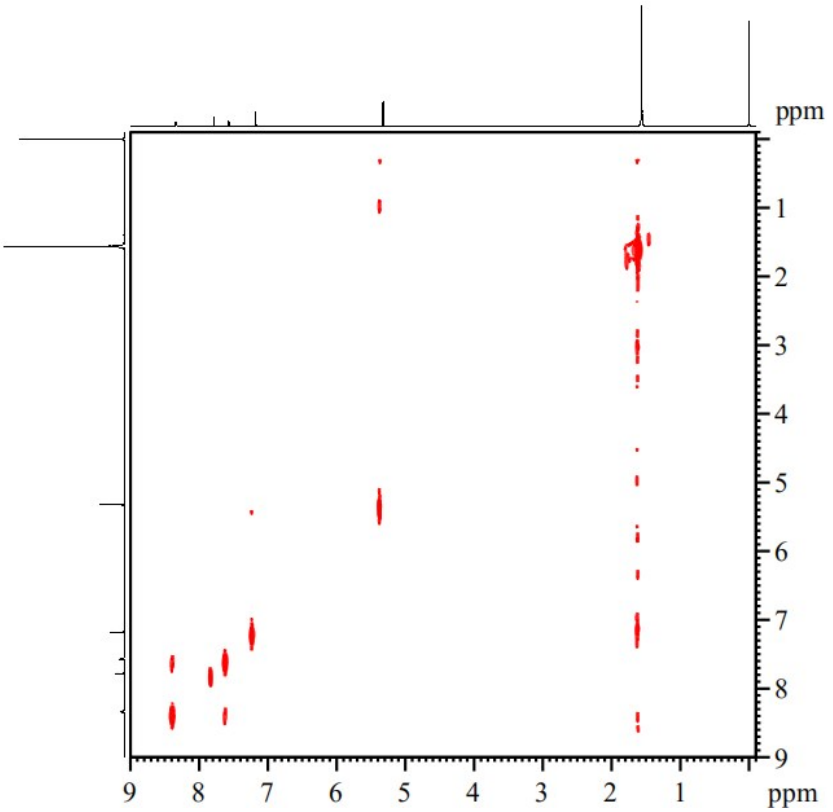

Figure S6. ^{1}H-^{1}H NOESY NMR spectrum of **1**.

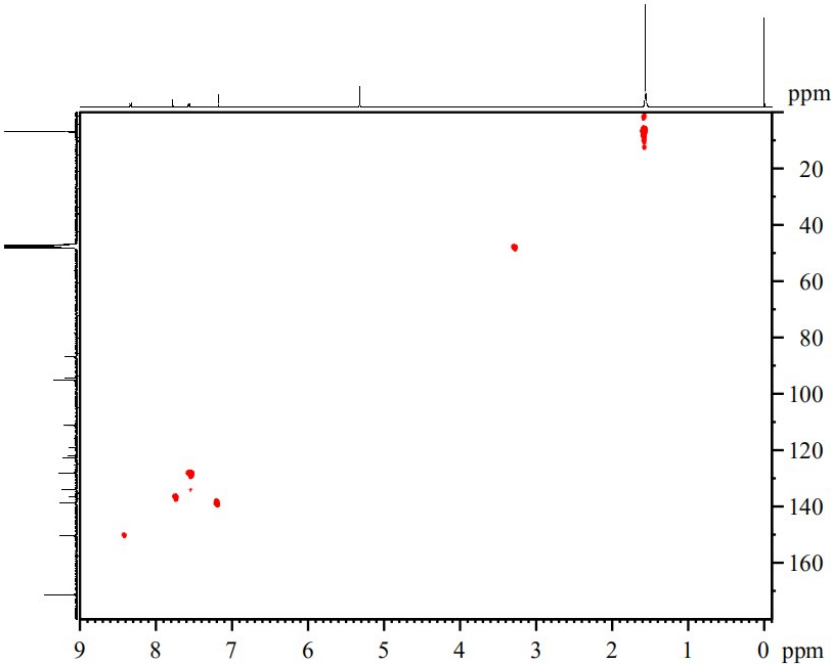

Figure S7. ^{1}H-^{13}C HSQC NMR spectrum of **1**.

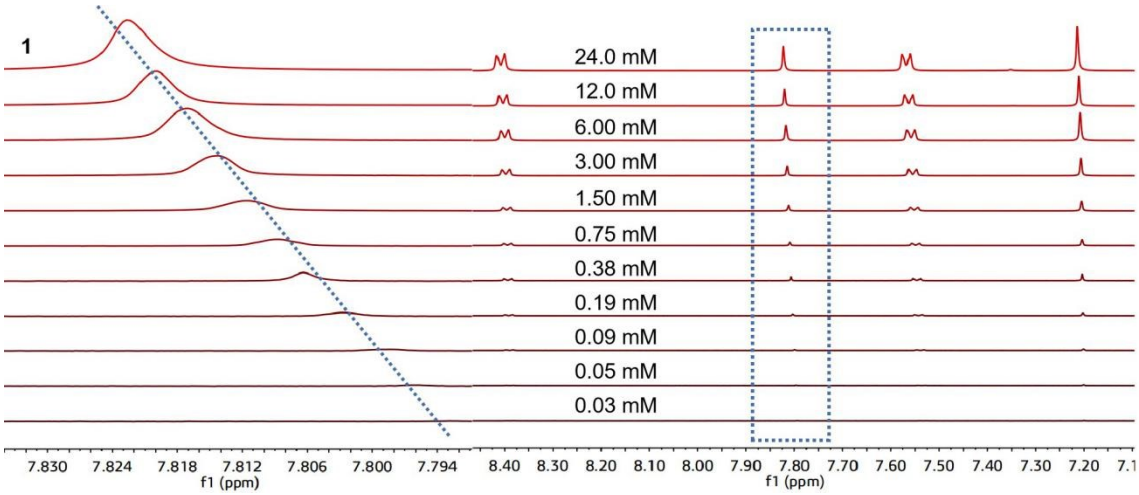

Figure S8. ^{1}H NMR spectra of **1** upon decreasing the concentration from 24.0 mM to 0.03 mM.

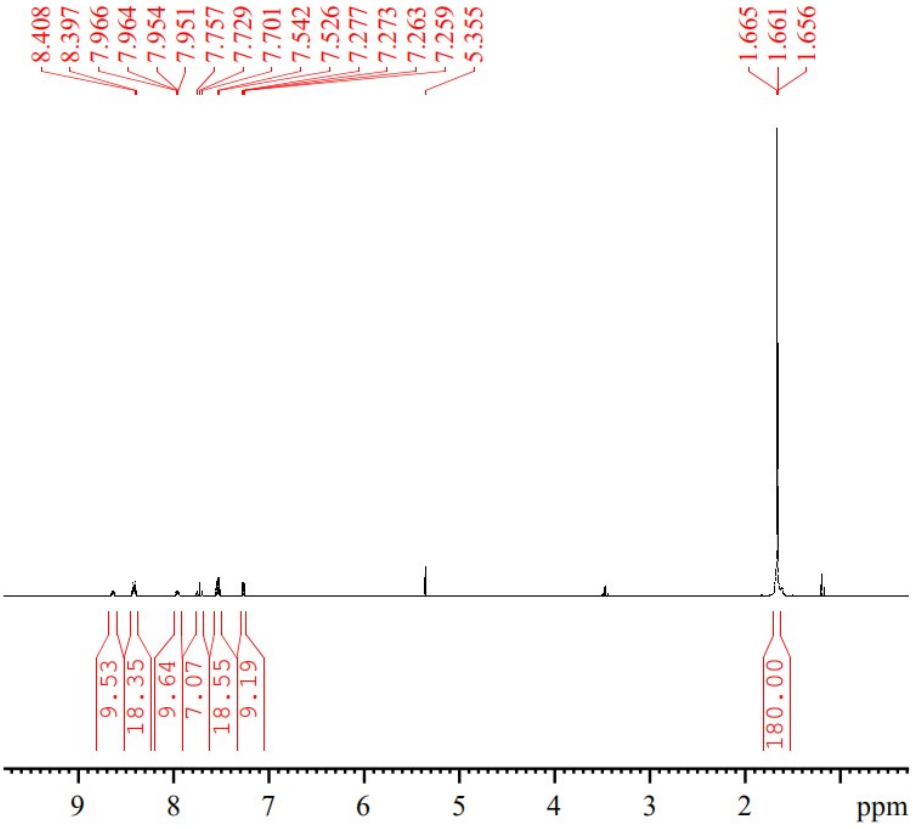

Figure S9. ^{1}H NMR spectrum of **2**.

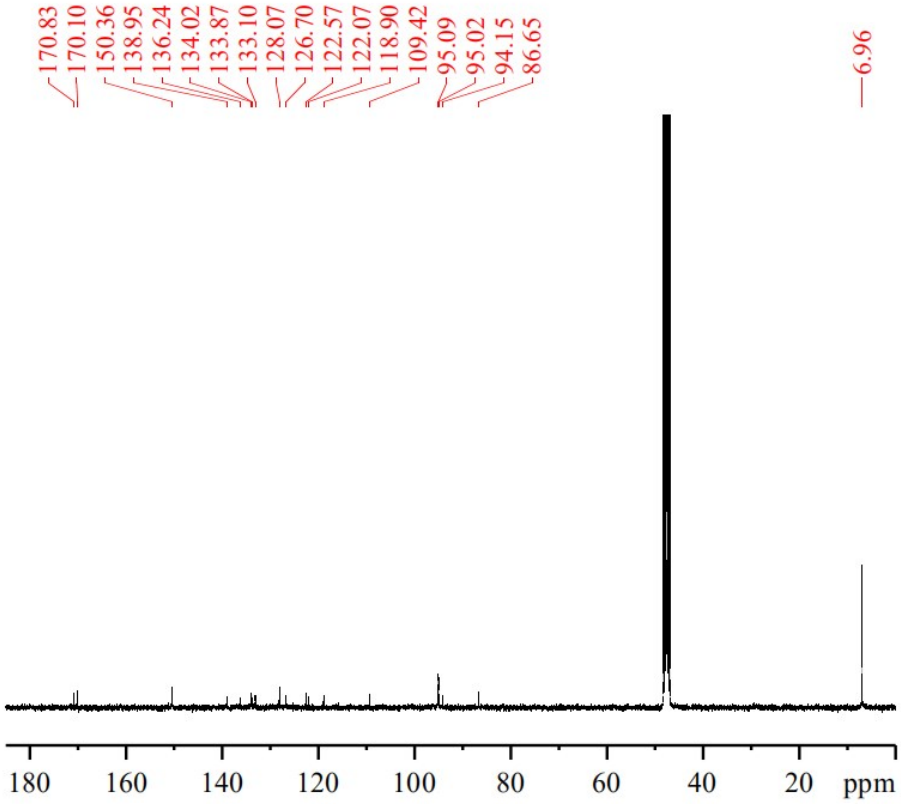

Figure S10. ^{13}C NMR spectrum of **2**.

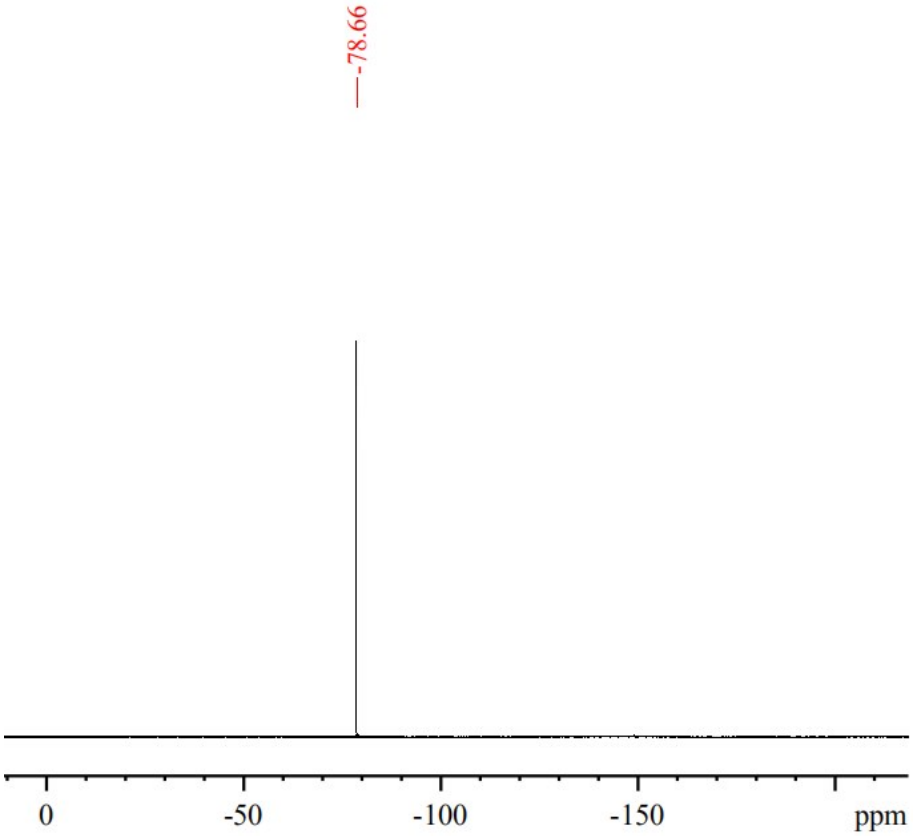

Figure S11. ^{19}F NMR spectrum of **2**.

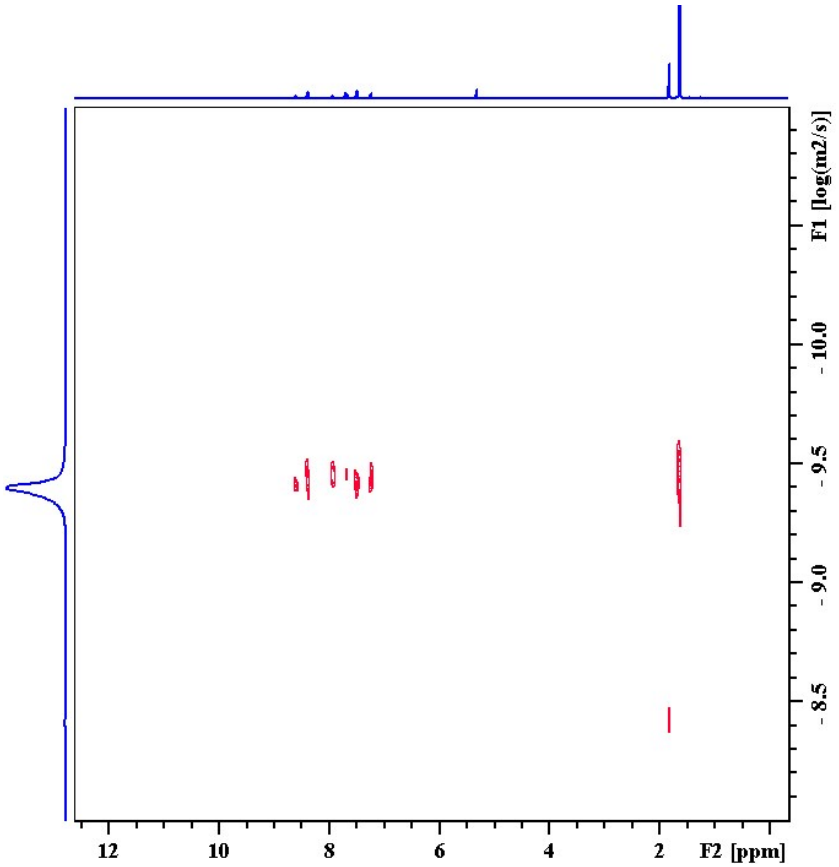

Figure S12. ^{1}H-^{1}H DOSY NMR spectrum of **2**.

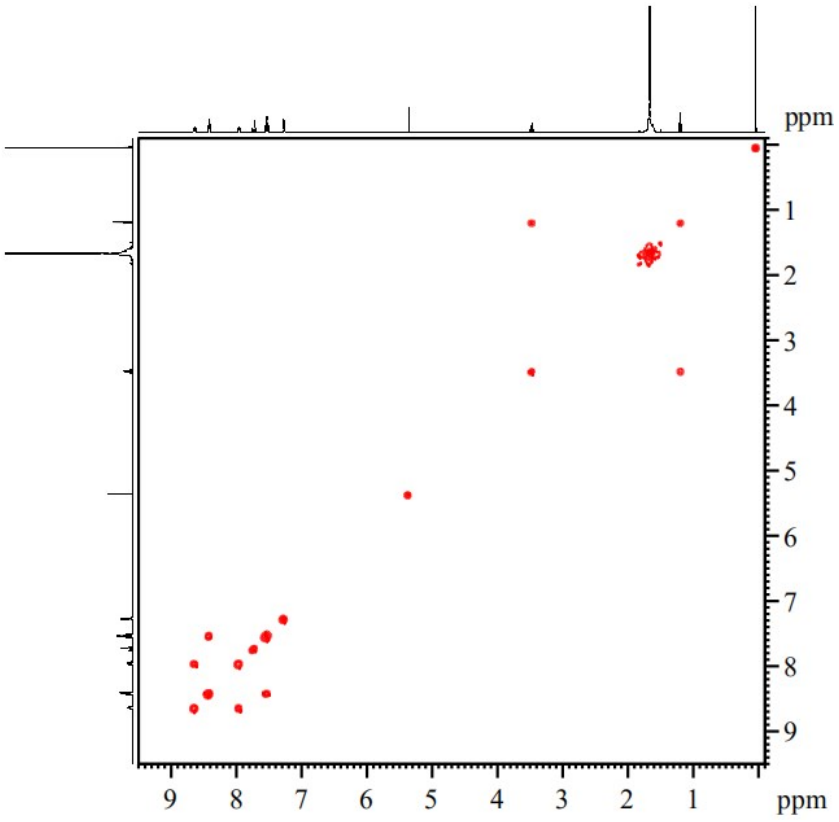

Figure S13. ^{1}H-^{1}H COSY NMR spectrum of **2**.

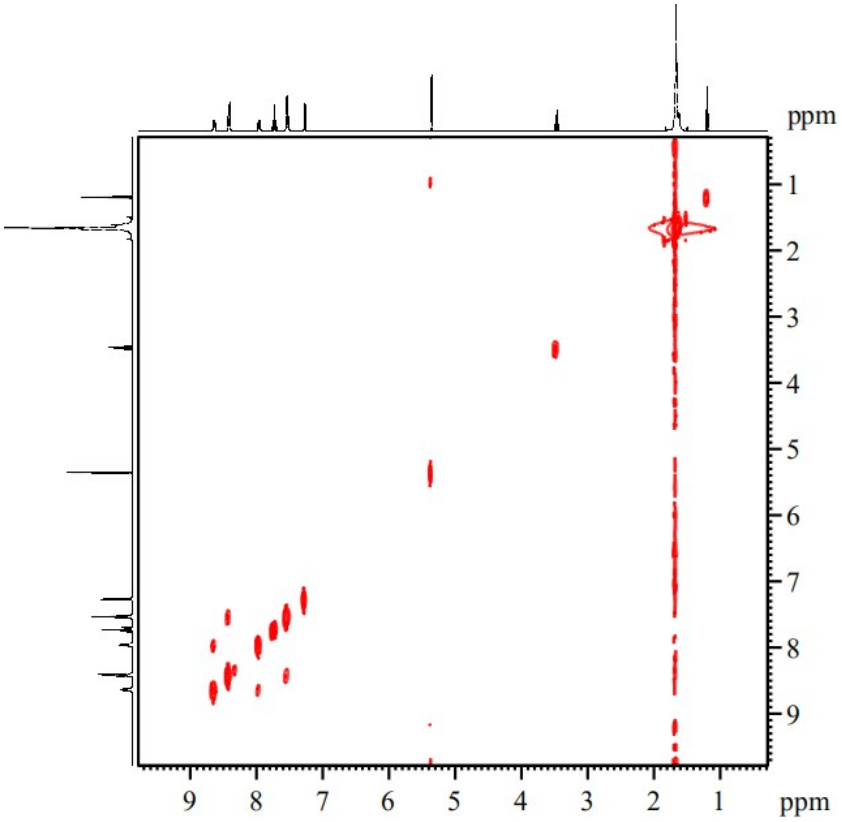

Figure S14. ^{1}H-^{1}H NOESY NMR spectrum of **2**.

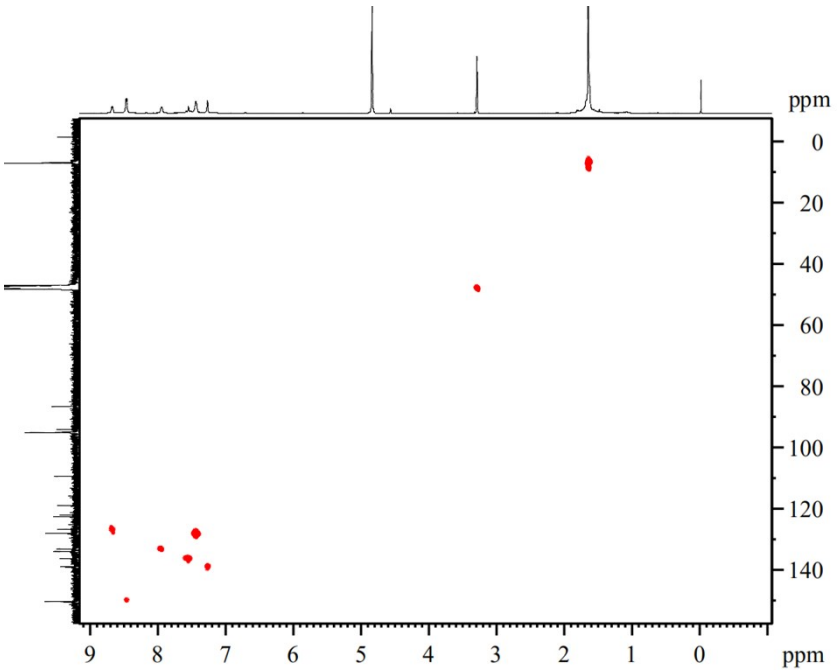

Figure S15. ^{1}H-^{13}C HSQC NMR spectrum of **2**.

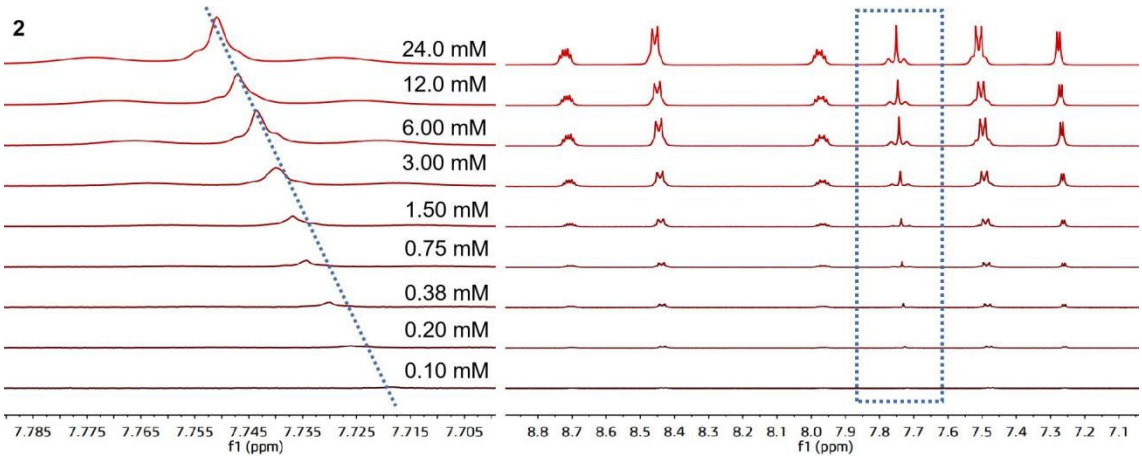

Figure S16. ^{1}H NMR spectra of **2** upon decreasing the concentration from 24.0 mM to 0.10 mM.

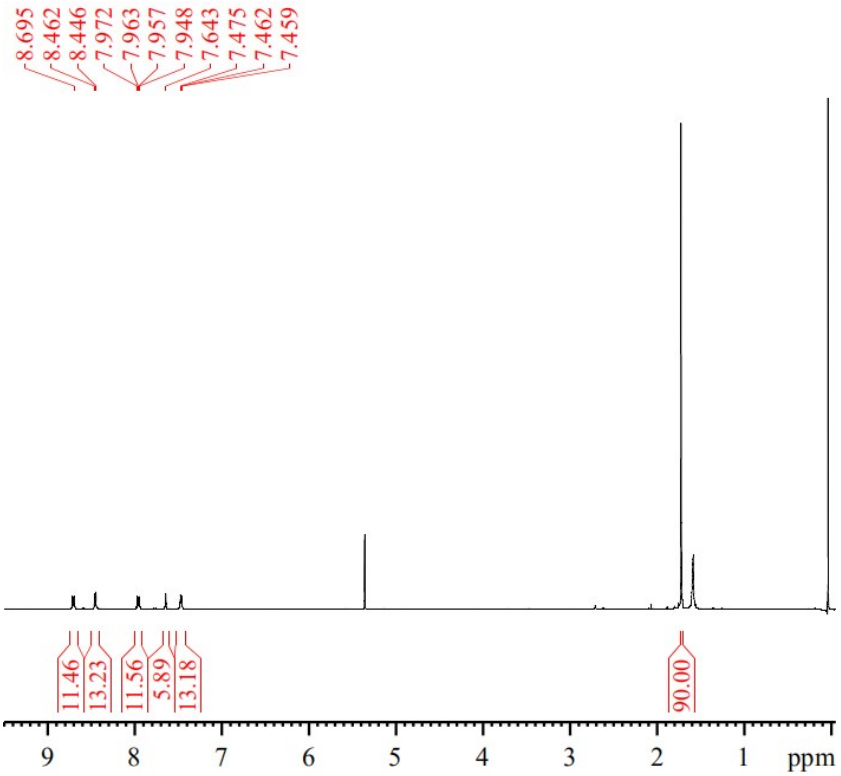

Figure S17. ^{1}H NMR spectrum of **3**.

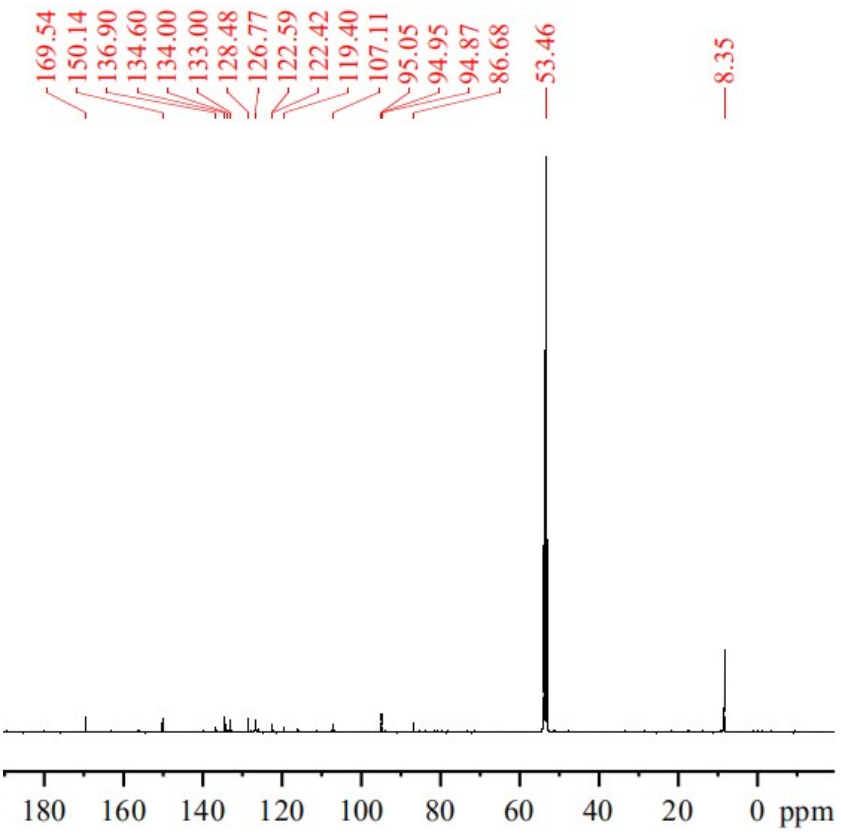

Figure S18. ^{13}C NMR spectrum of **3**.

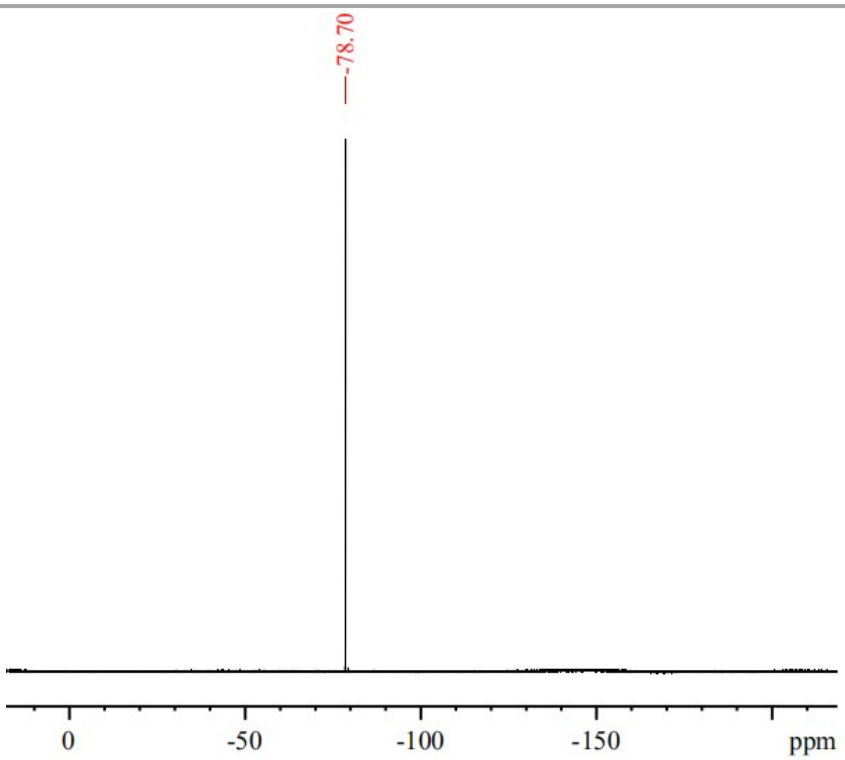

Figure S19. ^{19}F NMR spectrum of **3**.

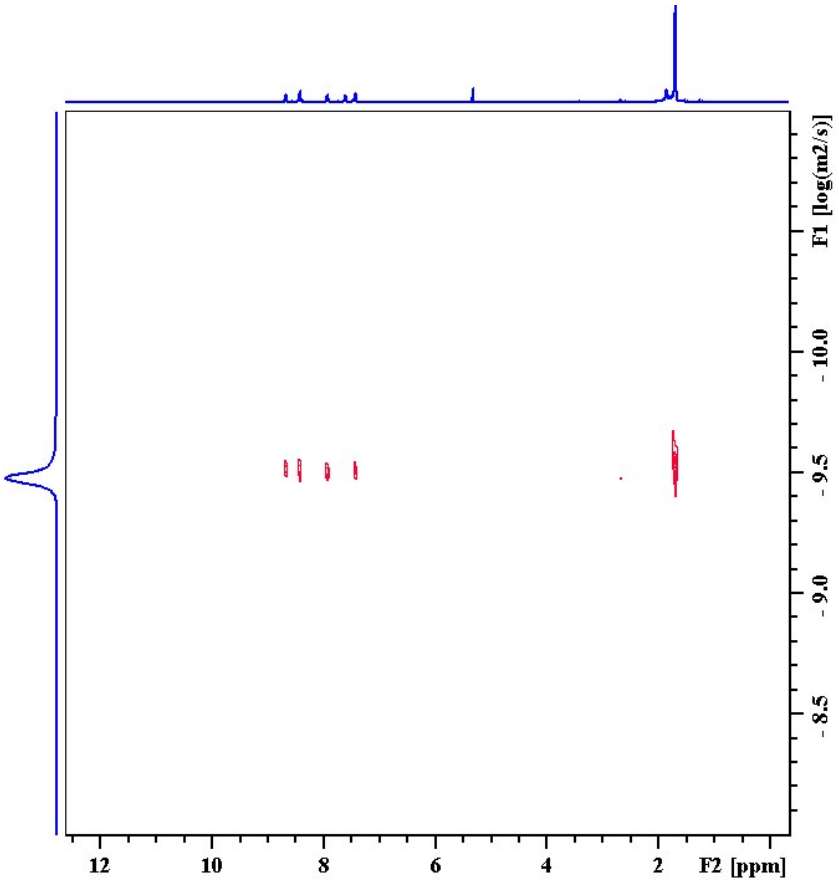

Figure S20. ^{1}H-^{1}H DOSY NMR spectrum of **3**.

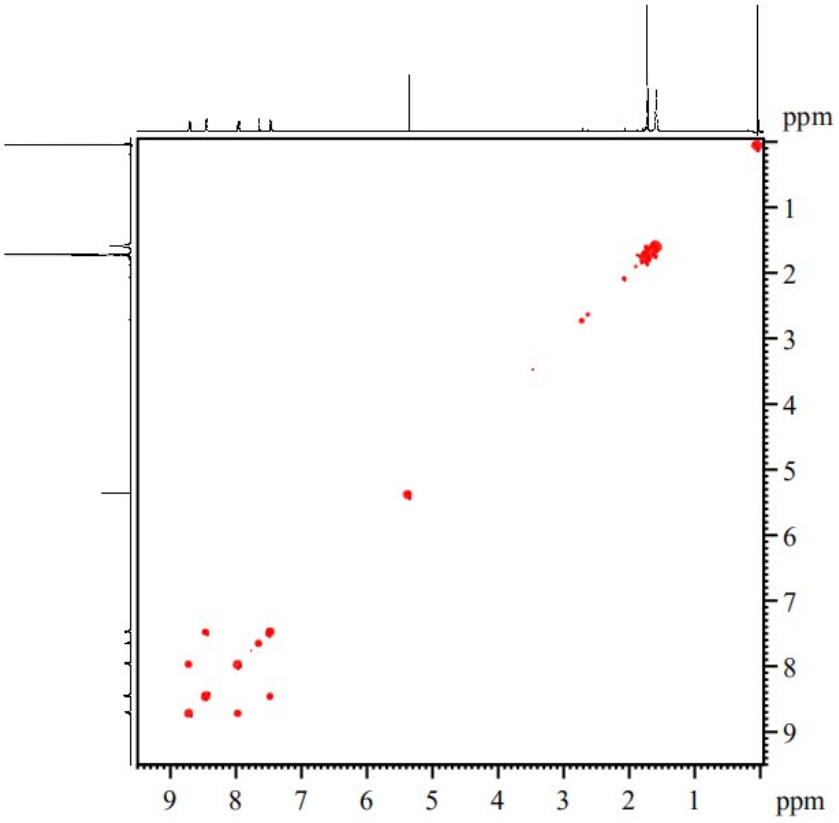

Figure S21. ^{1}H-^{1}H COSY NMR spectrum of **3**.

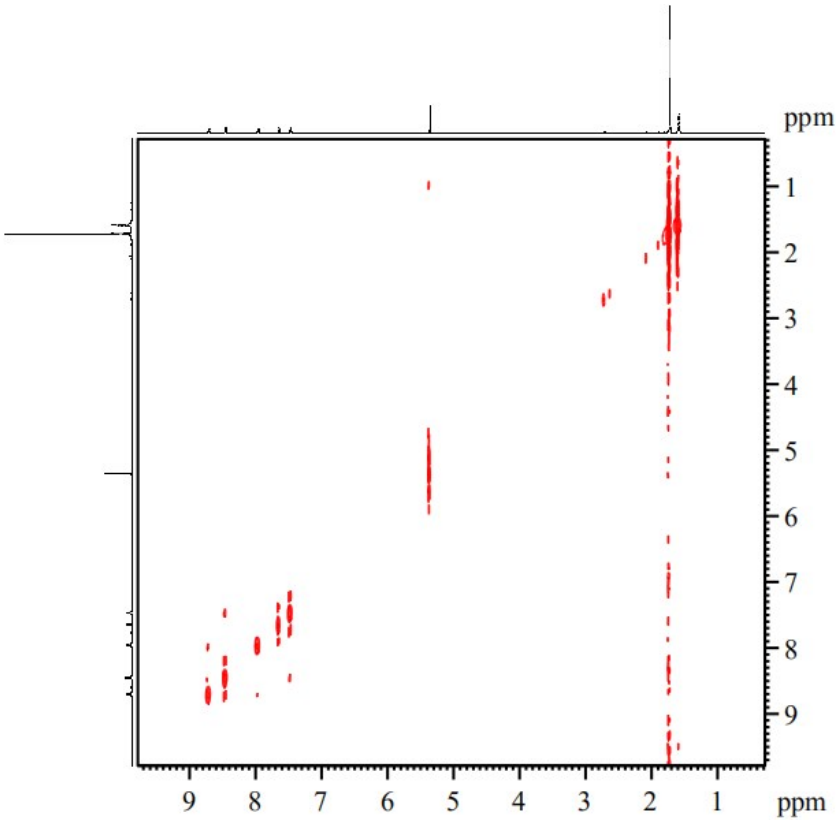

Figure S22. ^{1}H-^{1}H NOESY NMR spectrum of **3**.

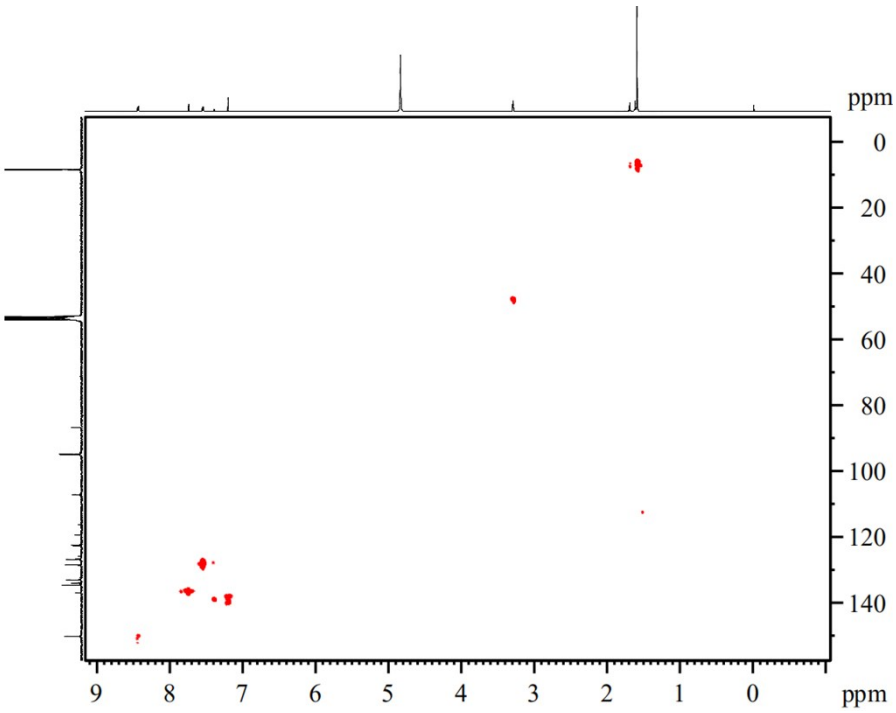

Figure S23. ^{1}H-^{13}C HSQC NMR spectrum of **3**.

2.2 UV spectra of host-guest assemblies

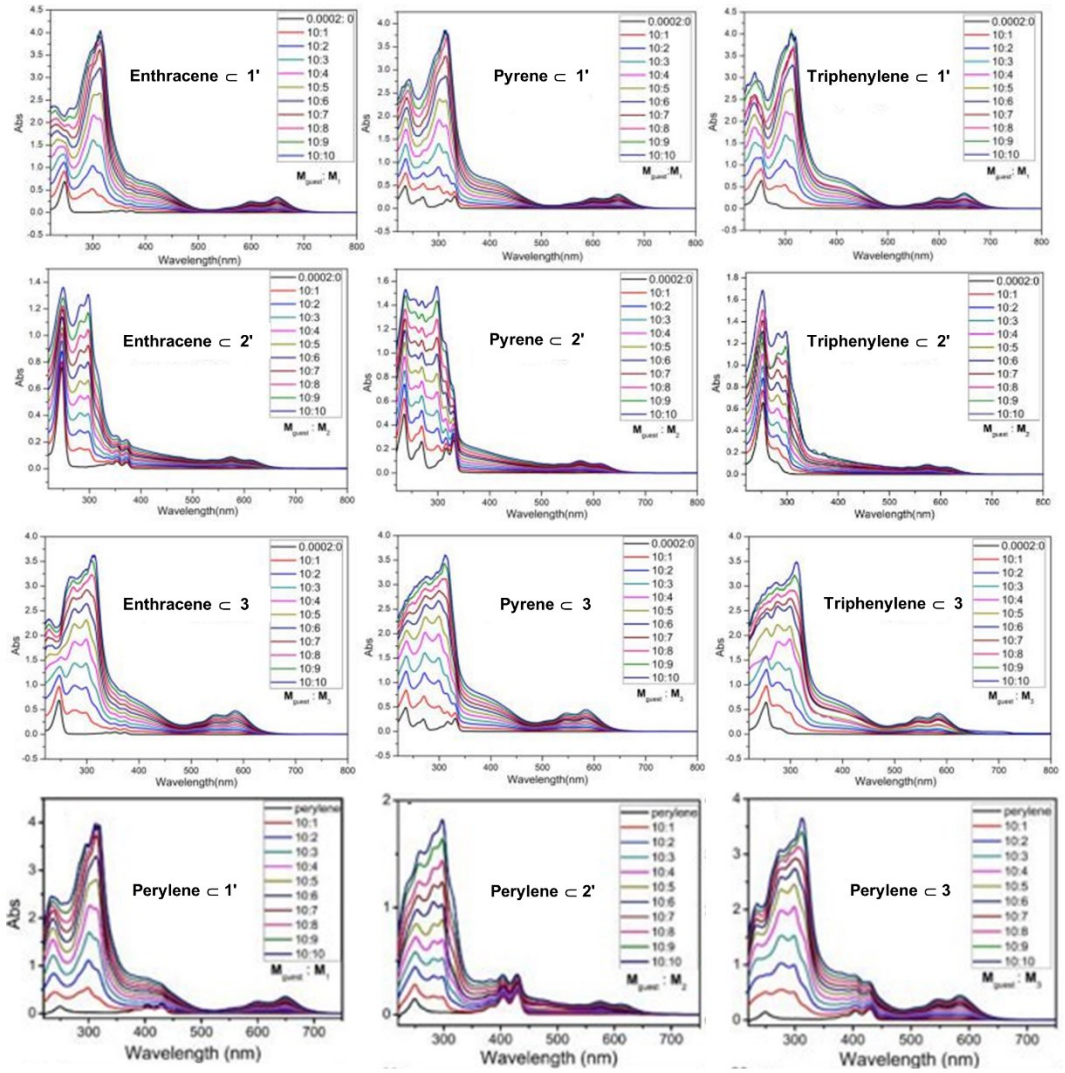

Figure S24. UV spectra of guest molecules encapsulated by complexes **1'**, **2'** and **3**.

2.3 Fluorescent spectra of host-guest assemblies

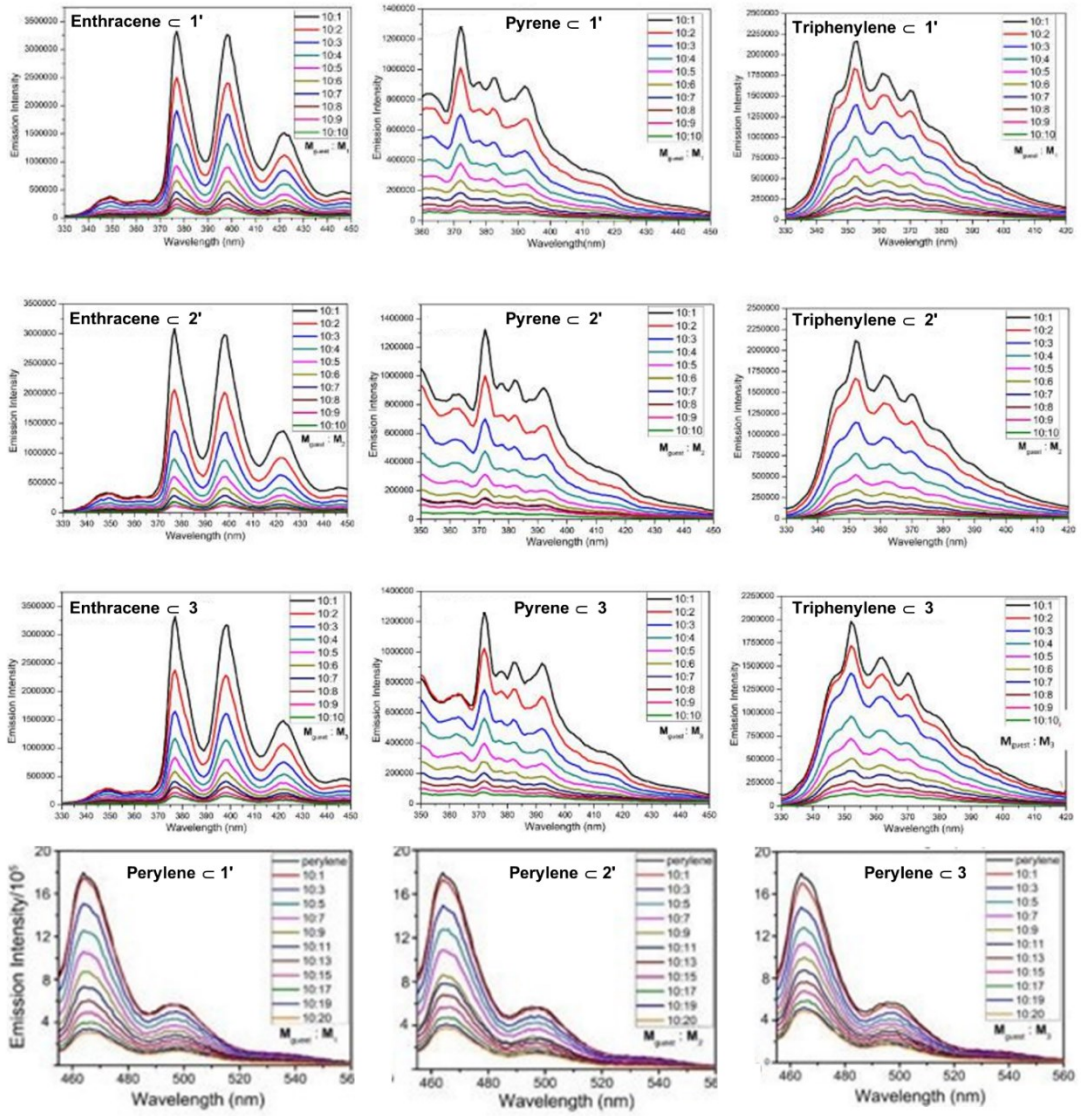

Figure S25. Fluorescent spectra of guest molecules encapsulated by complexes **1'**, **2'** and **3**.

2.4 ESI-TOF-MS spectra of 1, 2, 3 and their host-guest assemblies

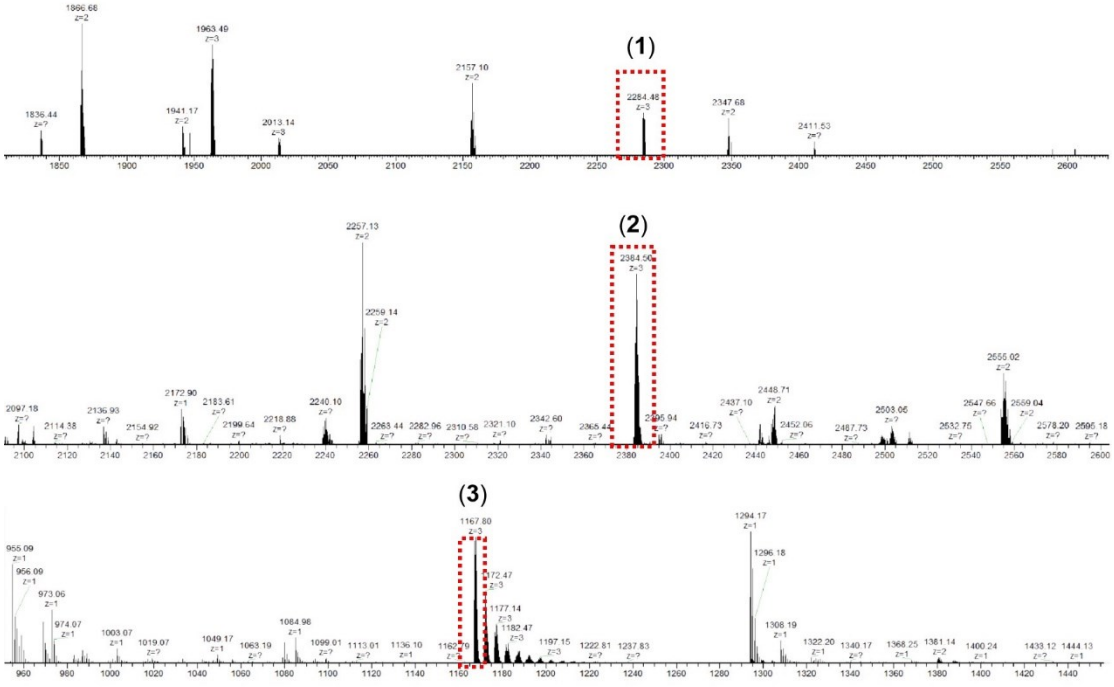

Figure S26. The full ESI-TOF-MS spectra of interlocked **1**, **2** and metallacage **3**.

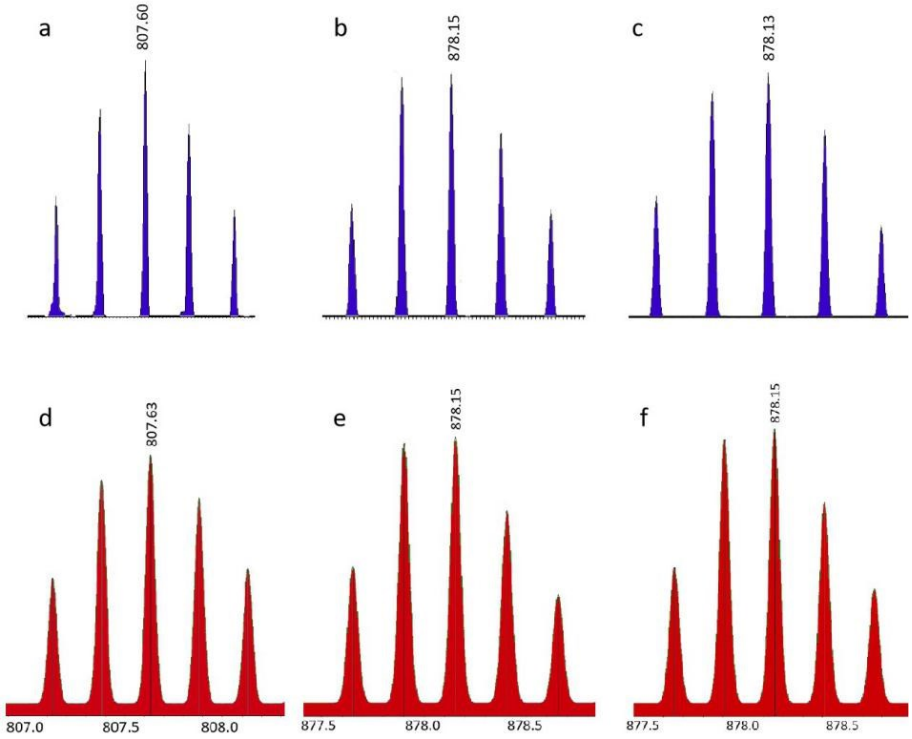

Figure S27. MS spectra of guest molecules encapsulated by **1** in CH_3OH. a) {[anthracene □ **1'**]-5OTf^-+Cl^- +6H_2O]}$^{4+}$+H^+; b) {[pyrene □ **1'**]-4OTf^-+8CH_3OH]}$^{4+}$; c){[triphenylene □**1'**]+2CH_3OH+2$CH_3CH_2OCH_2CH_3$+H_2O-4OTf^-}$^{4+}$; d), e), and f) are simulated for a), b) and c), respectively.

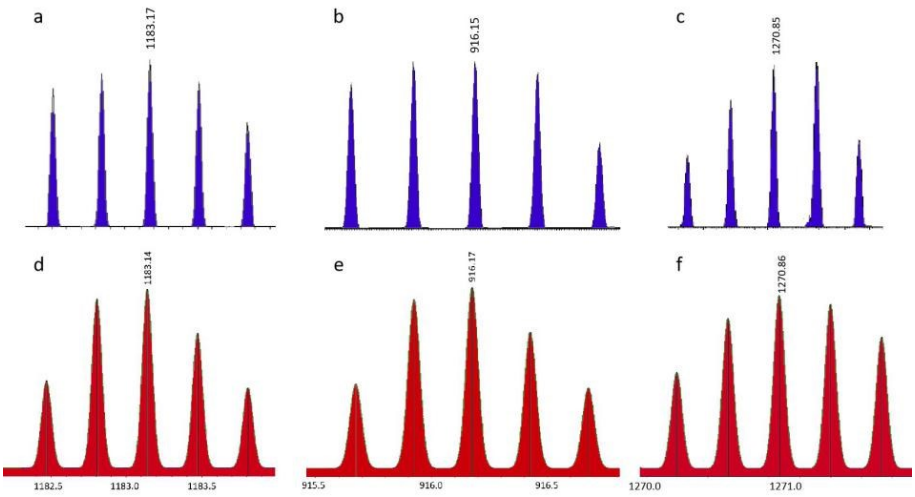

Figure S28. MS spectra of guest molecules encapsulated by **2** in CH_3OH and CD_3OD. a) {[anthracene □ **2'**]-3OTf$^-$+H_2O]}$^{3+}$; b) {[pyrene □ **2'**]-4OTf$^-$ + 2CD_3OD + 5H_2O + 3CH_3OH]}$^{4+}$; c){[triphenylene □**2'**]+8CH_3OH+H_2O-3OTf$^-$}$^{4+}$ + Cl^-; d), e), and f) are simulated for a), b) and c), respectively.

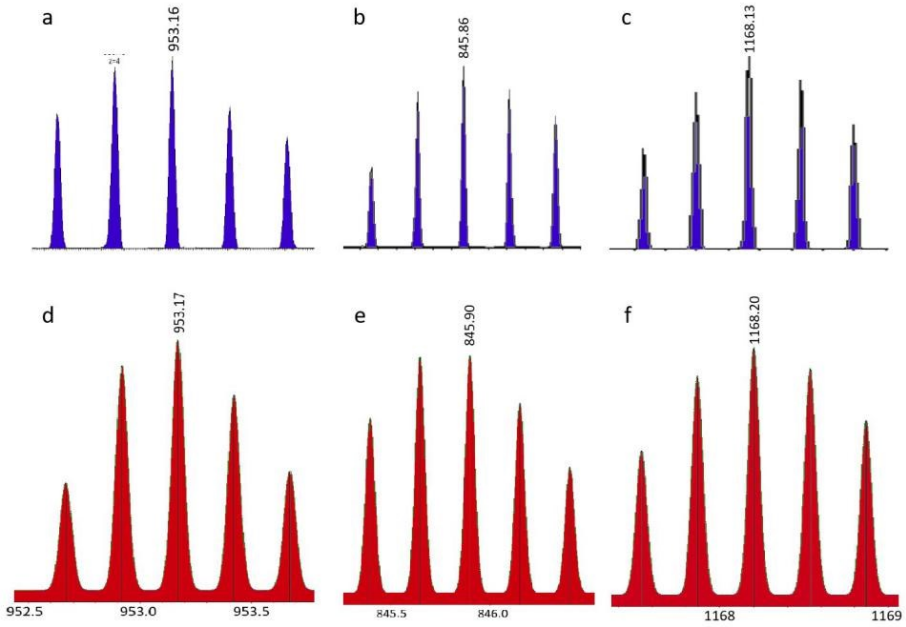

Figure S29. MS spectra of guest molecules encapsulated by **3** in CH_3OH and CD_3OD. a) {[anthracene □ **3**]-$4OTf^- + 2CH_3OH + 12H_2O$]}$^{4+}$; b) {[pyrene □ **3**] + $2Cl^-$ + CD_3OD + H_2O - $6OTf^-$]}$^{4+}$; c){[triphenylene □**3**] + $3Cl^-$ + $3CH_3OH$+H_2O-$6OTf^-$}$^{3+}$; d), e), and f) are simulated for a), b) and c), respectively.

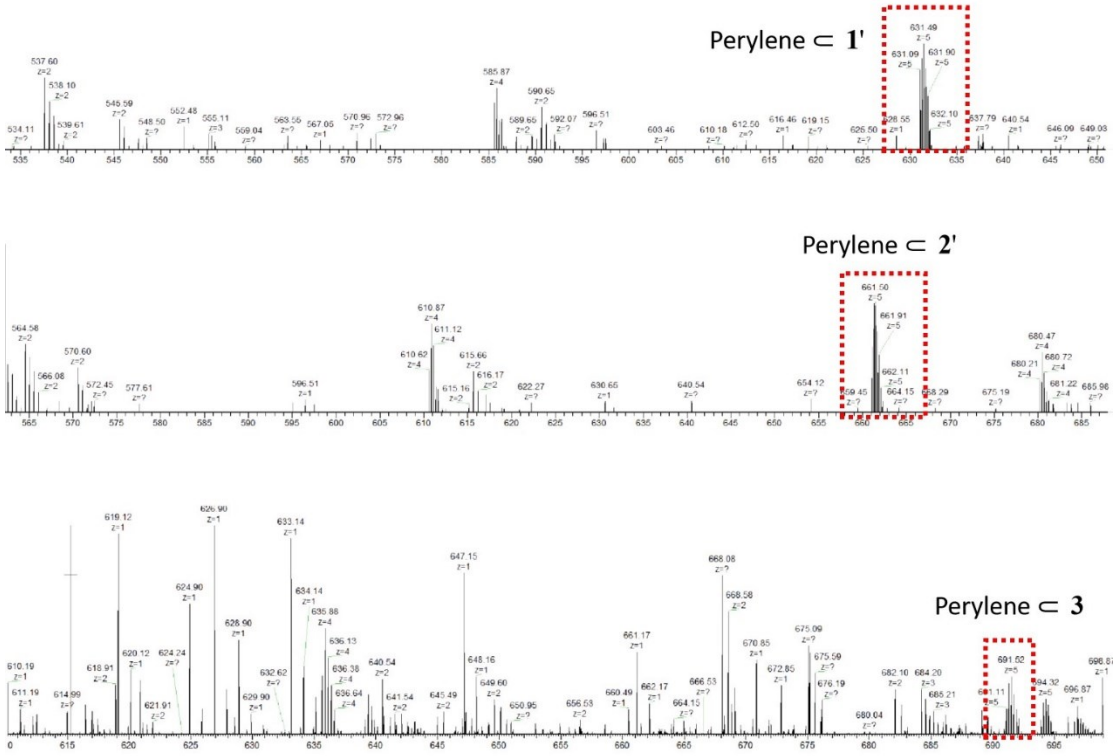

Figure S30. The full ESI-TOF-MS spectra of perylene encapsulated by **1'**, **2'** and **3**.

2.5 NMR spectra of host-guest assemblies

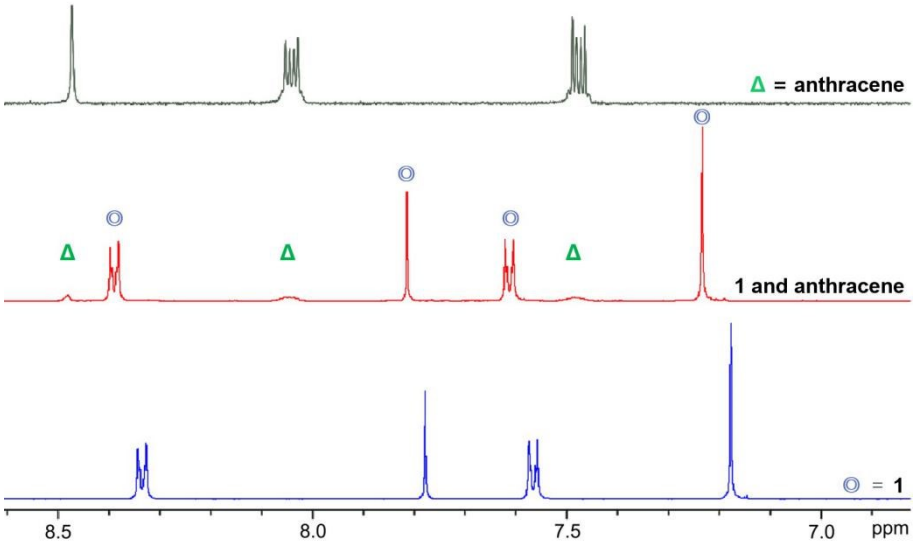

Figure S31. The ^{1}H NMR spectra of anthracene encapsulated by **1** in CD_3OD.

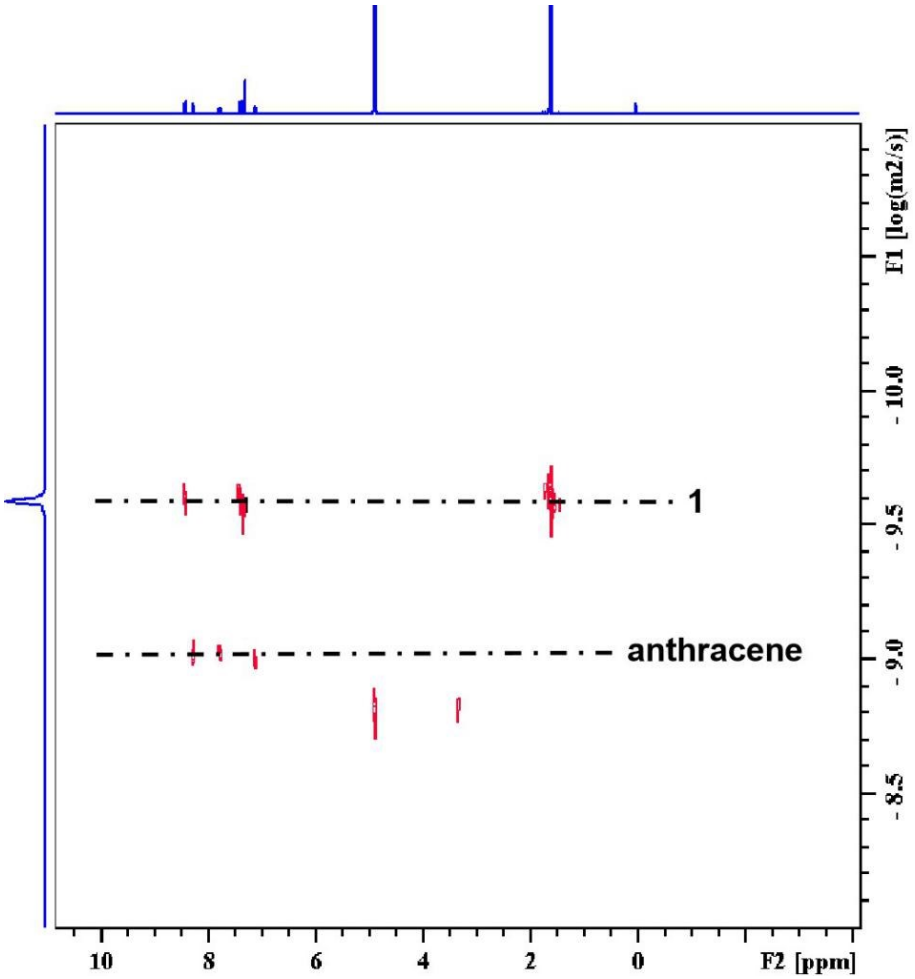

Figure S32. The ^{1}H-^{1}H DOSY NMR spectra of anthracene encapsulated by **1** in CD_3OD.

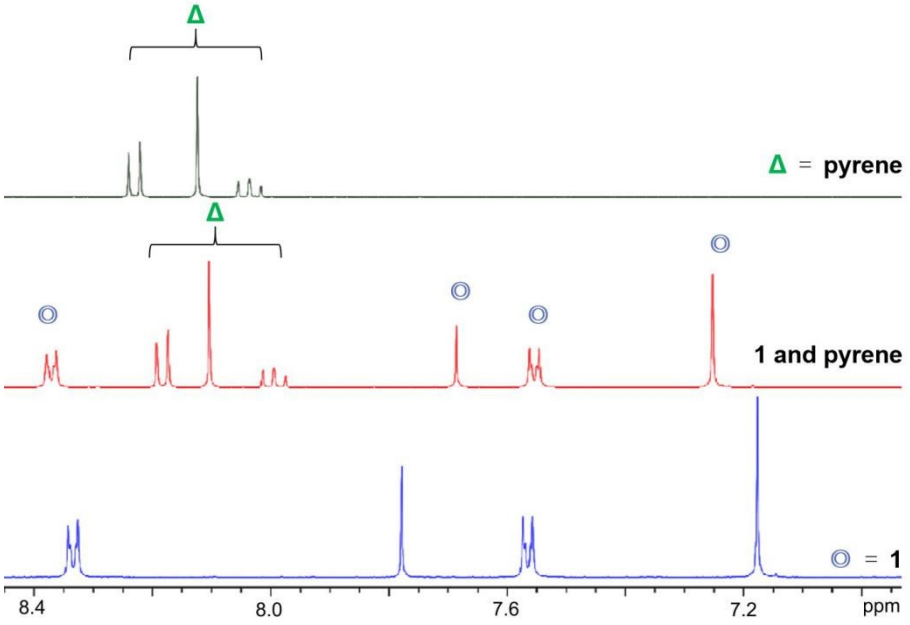

Figure S33. The ^{1}H NMR spectra of pyrene encapsulated by **1** in CD_3OD.

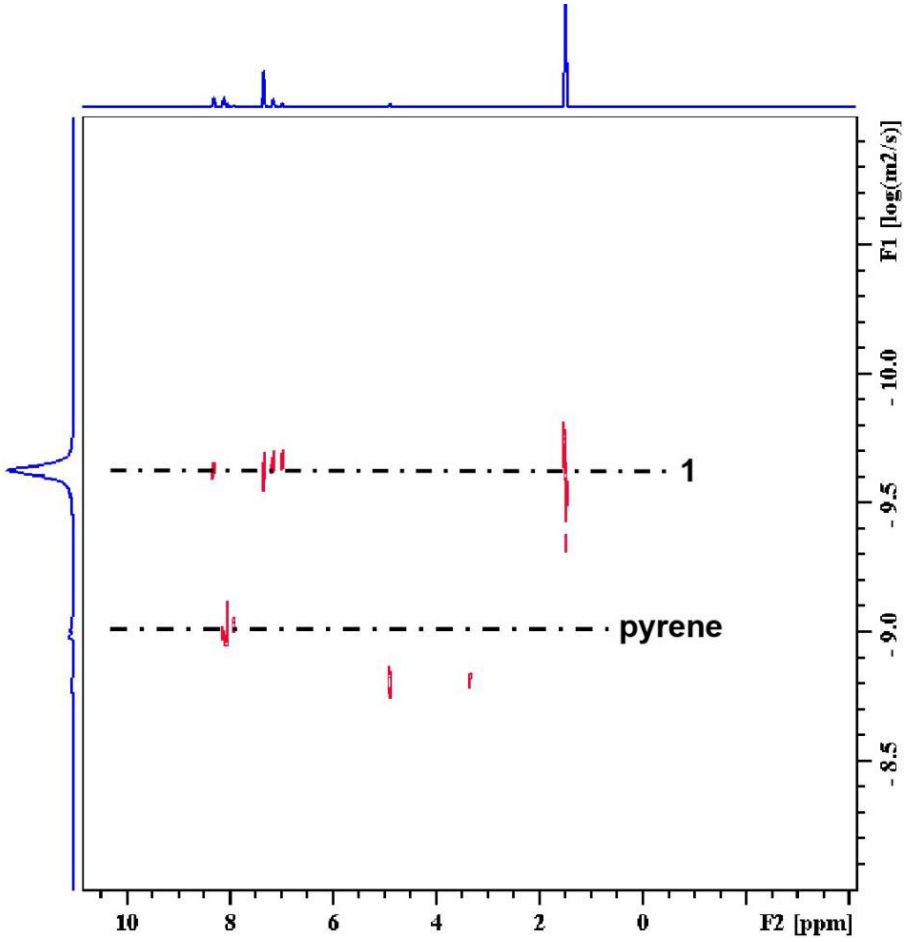

Figure S34. The ^{1}H-^{1}H DOSY NMR spectra of pyrene encapsulated by **1** in CD_3OD.

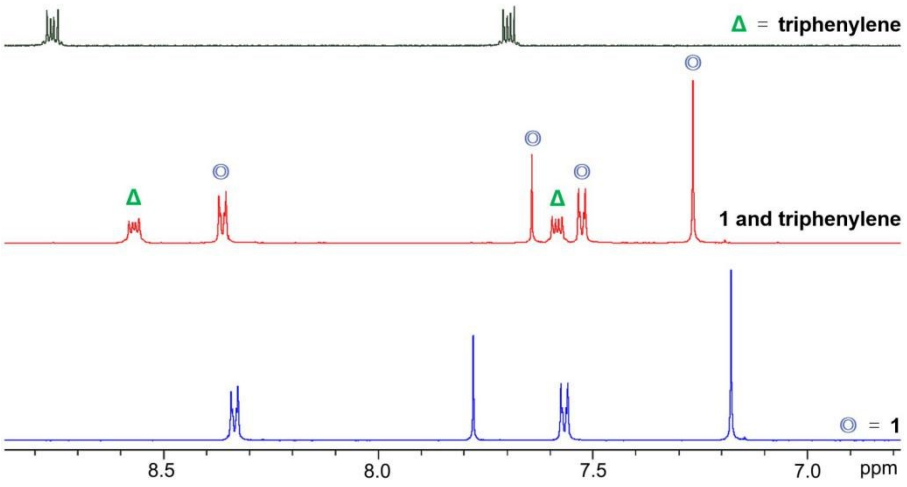

Figure S35. The ^{1}H NMR spectra of triphenylene encapsulated by **1** in CD_3OD.

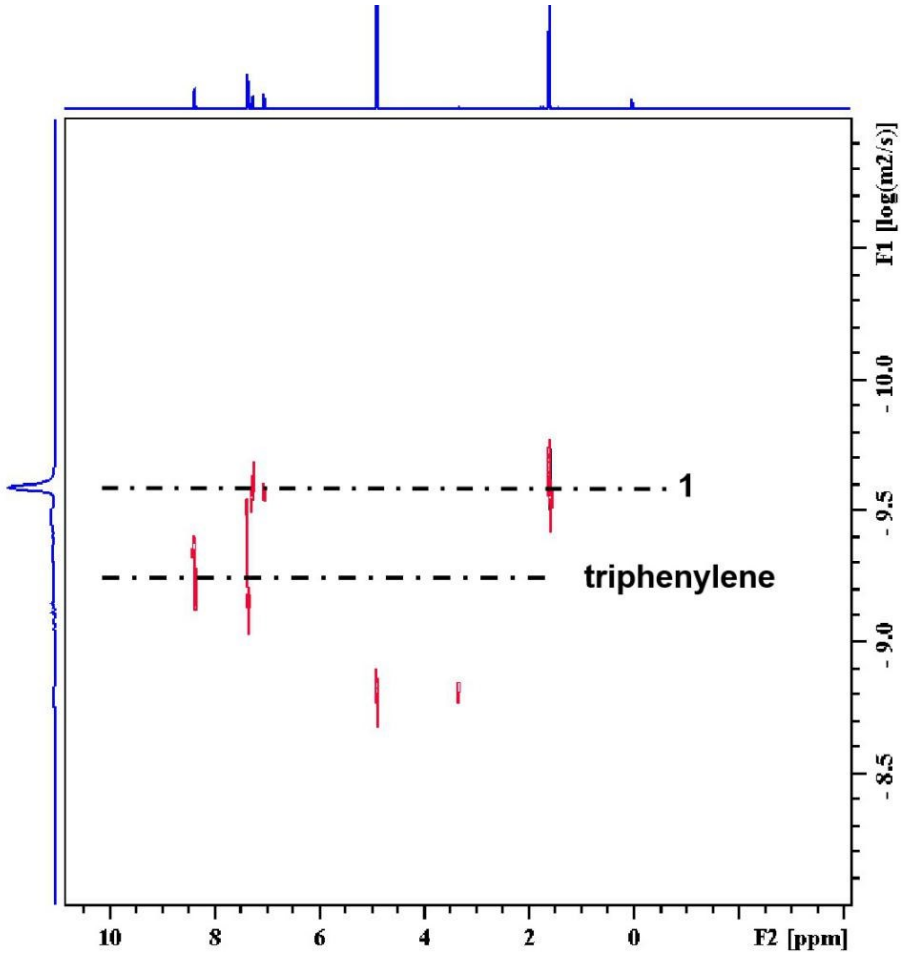

Figure S36. The ^{1}H-^{1}H DOSY NMR spectra of triphenylene encapsulated by **1** in CD_3OD.

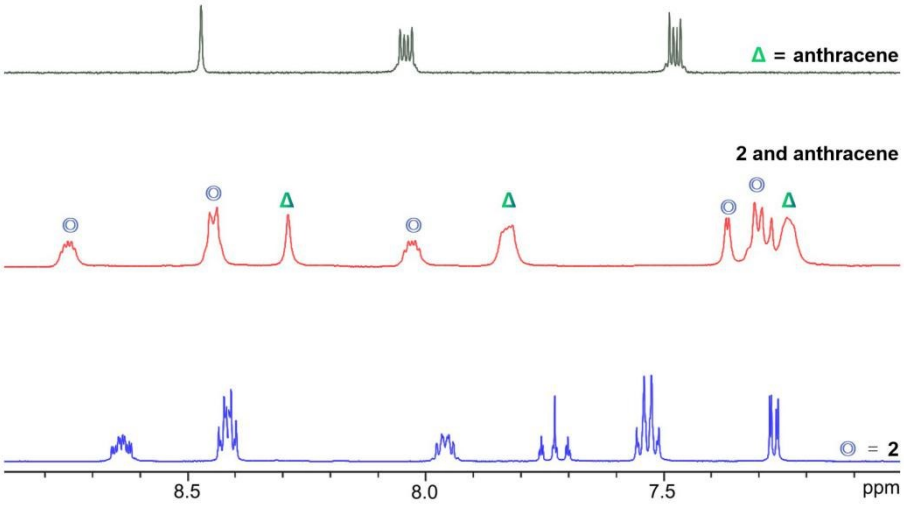

Figure S37. The ^{1}H NMR spectra of anthracene encapsulated by **2** in CD_3OD.

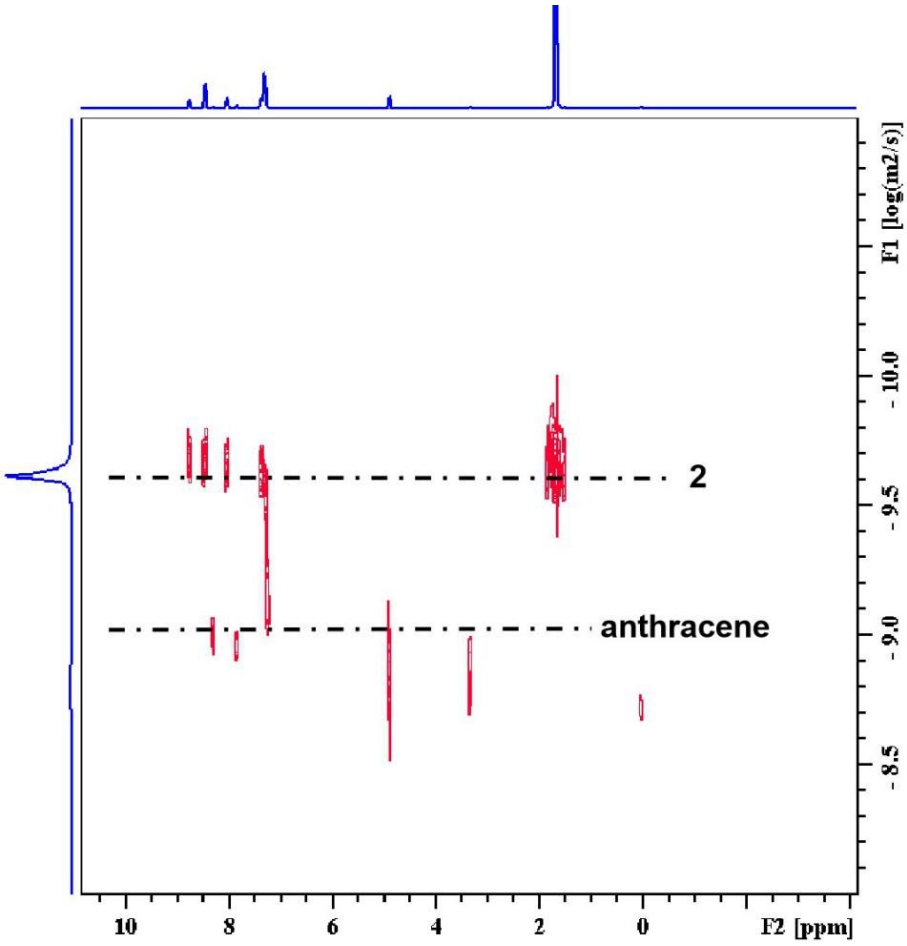

Figure S38. The ^{1}H-^{1}H DOSY NMR spectra of anthracene encapsulated by **2** in CD_3OD.

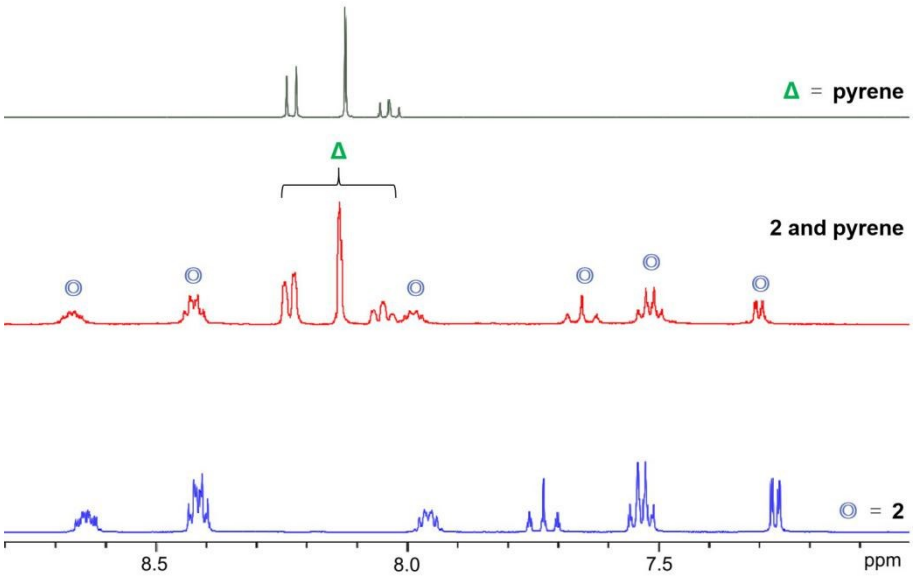

Figure S39. The ^{1}H NMR spectra of pyrene encapsulated by **2** in CD_3OD.

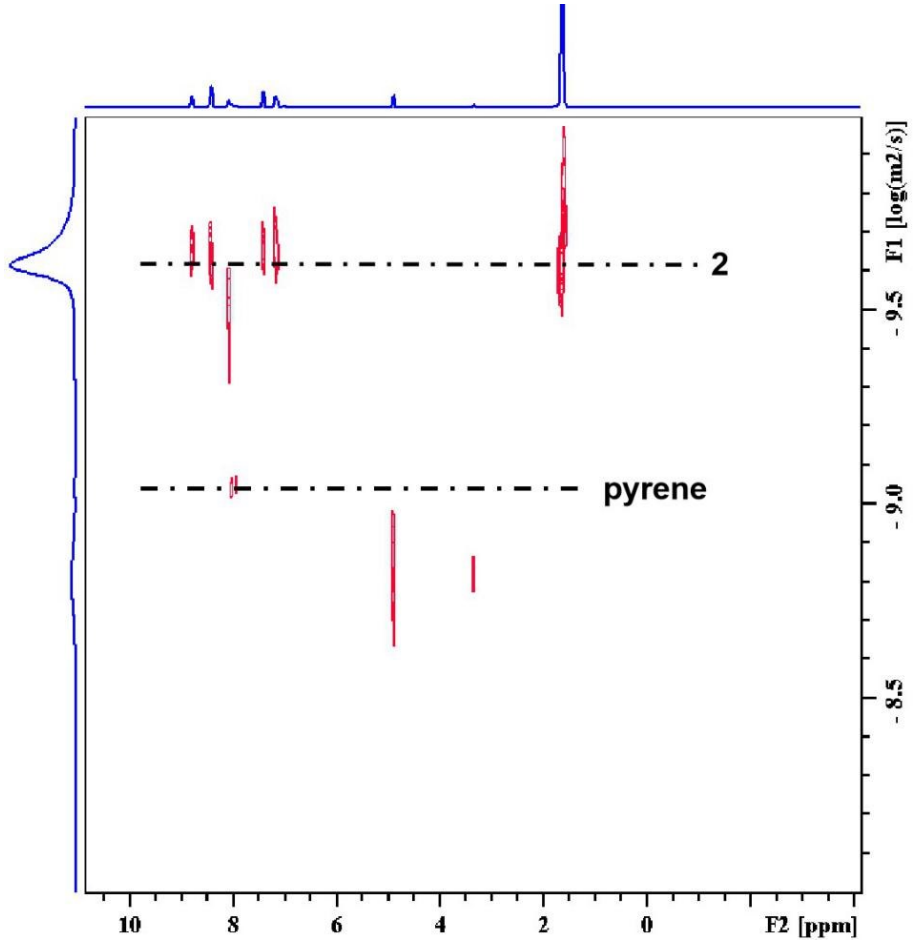

Figure S40. The ^{1}H-^{1}H DOSY NMR spectra of pyrene encapsulated by **2** in CD_3OD.

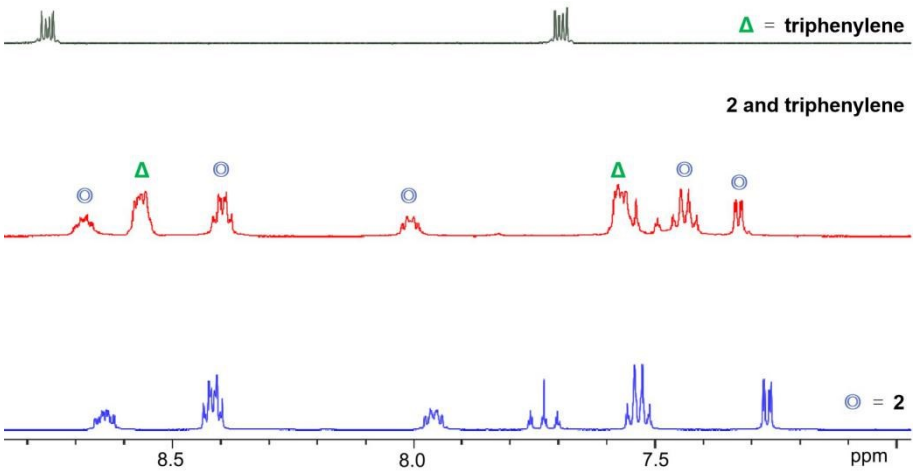

Figure S41. The ^{1}H NMR spectra of triphenylene encapsulated by **2** in CD_3OD.

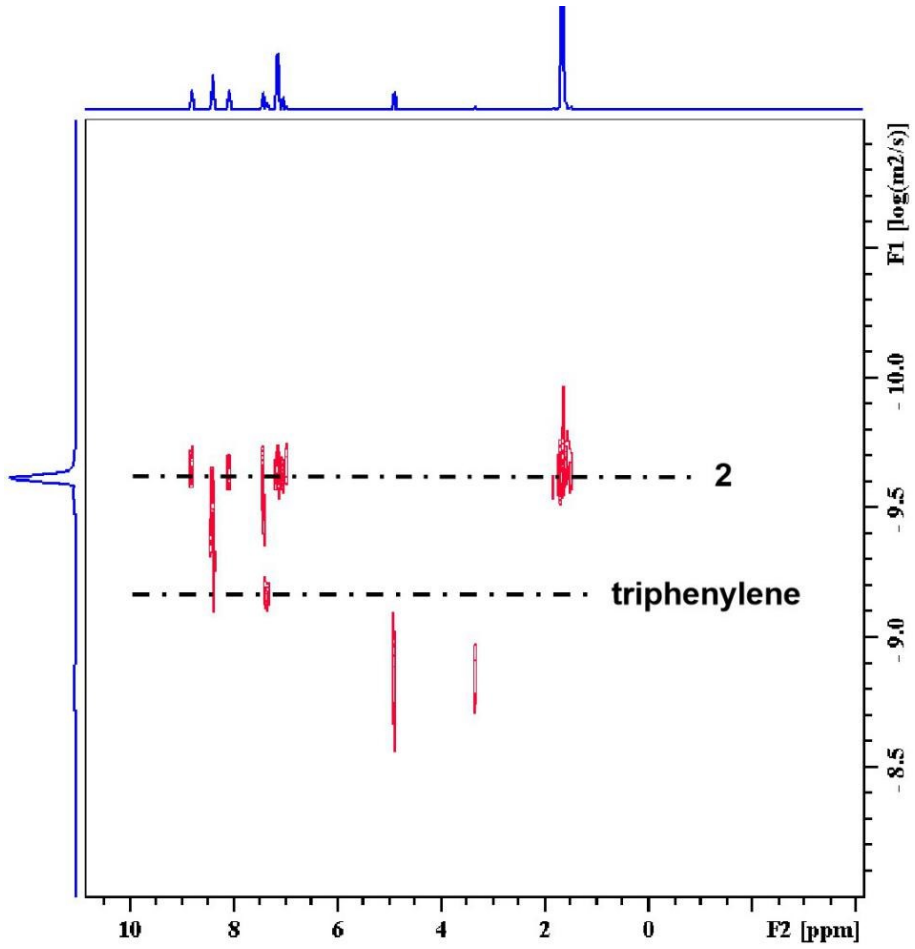

Figure S42. The ^{1}H-^{1}H DOSY NMR spectra of triphenylene encapsulated by **2** in CD_3OD.

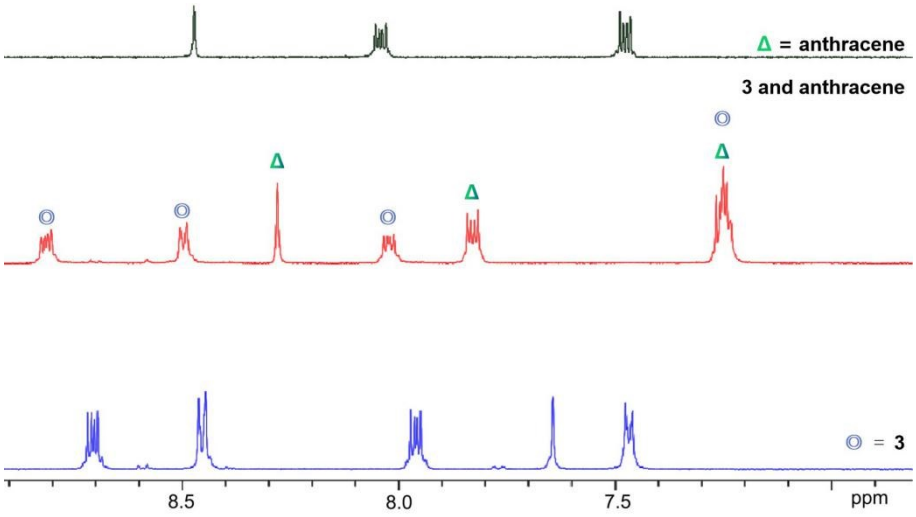

Figure S43. The ^{1}H NMR spectra of anthracene encapsulated by **3** in CD_3OD.

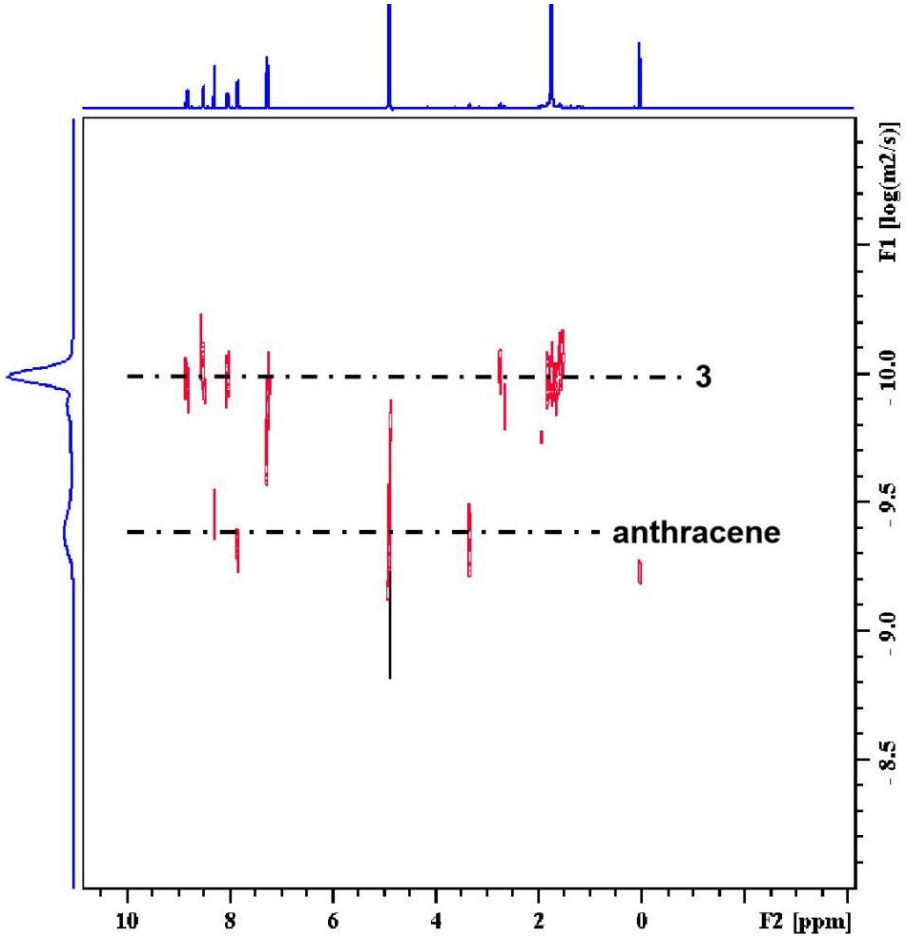

Figure S44. The ^{1}H-^{1}H DOSY NMR spectra of anthracene encapsulated by **3** in CD_3OD.

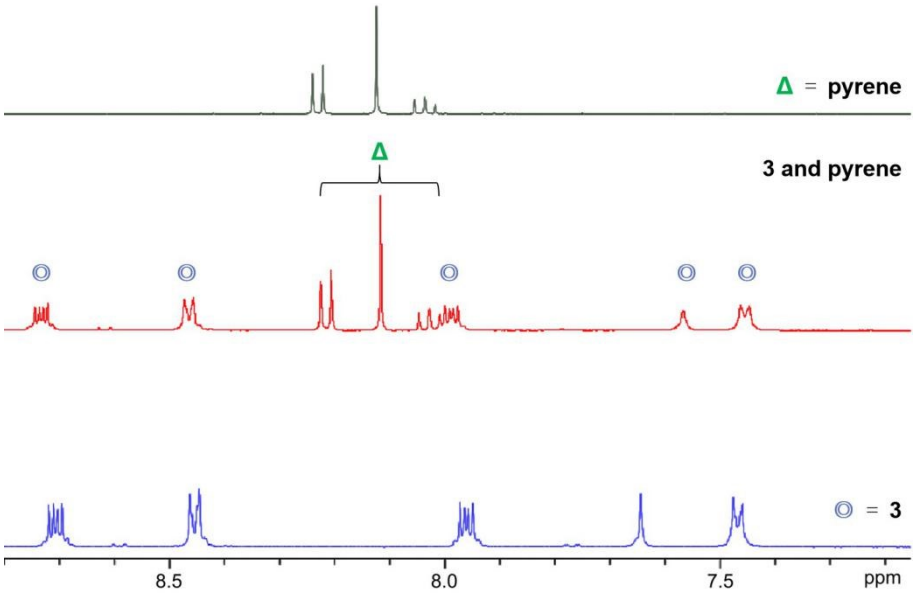

Figure S45. The ^{1}H NMR spectra of pyrene encapsulated by **3** in CD_3OD.

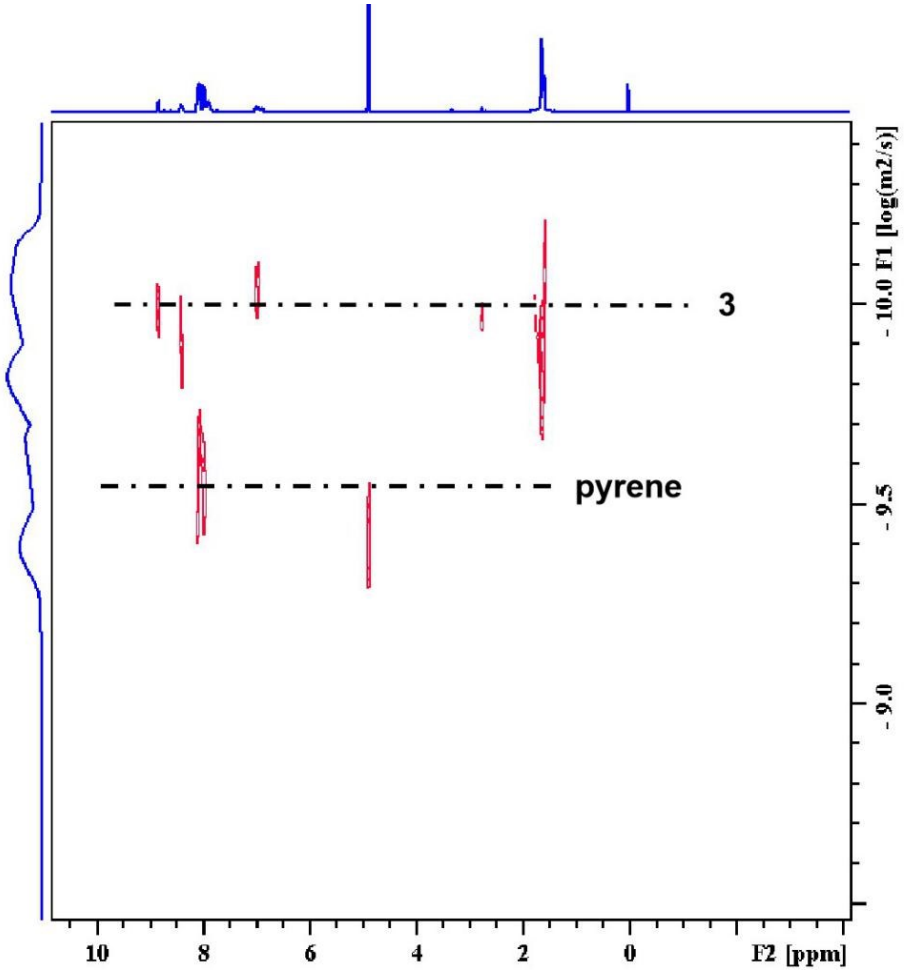

Figure S46. The ^{1}H-^{1}H DOSY NMR spectra of pyrene encapsulated by **3** in CD_3OD.

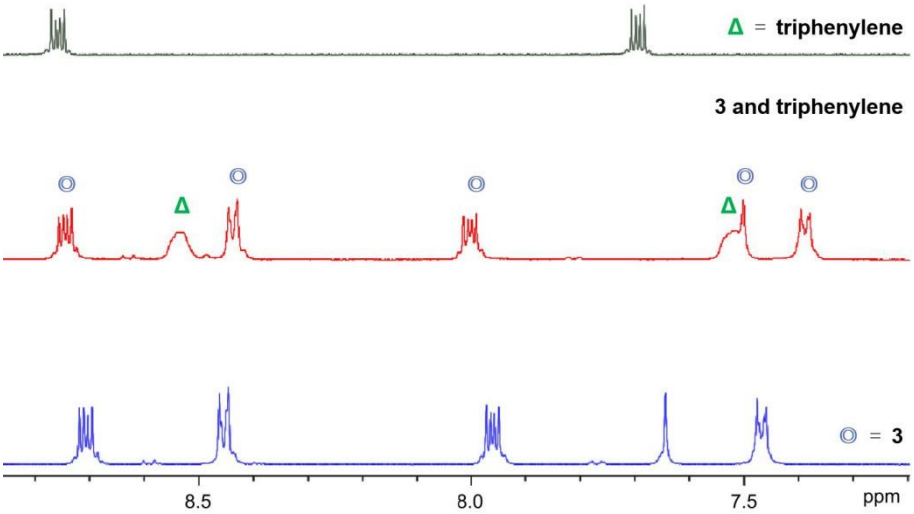

Figure S47. The ^{1}H NMR spectra of triphenyene encapsulated by **3** in CD_3OD.

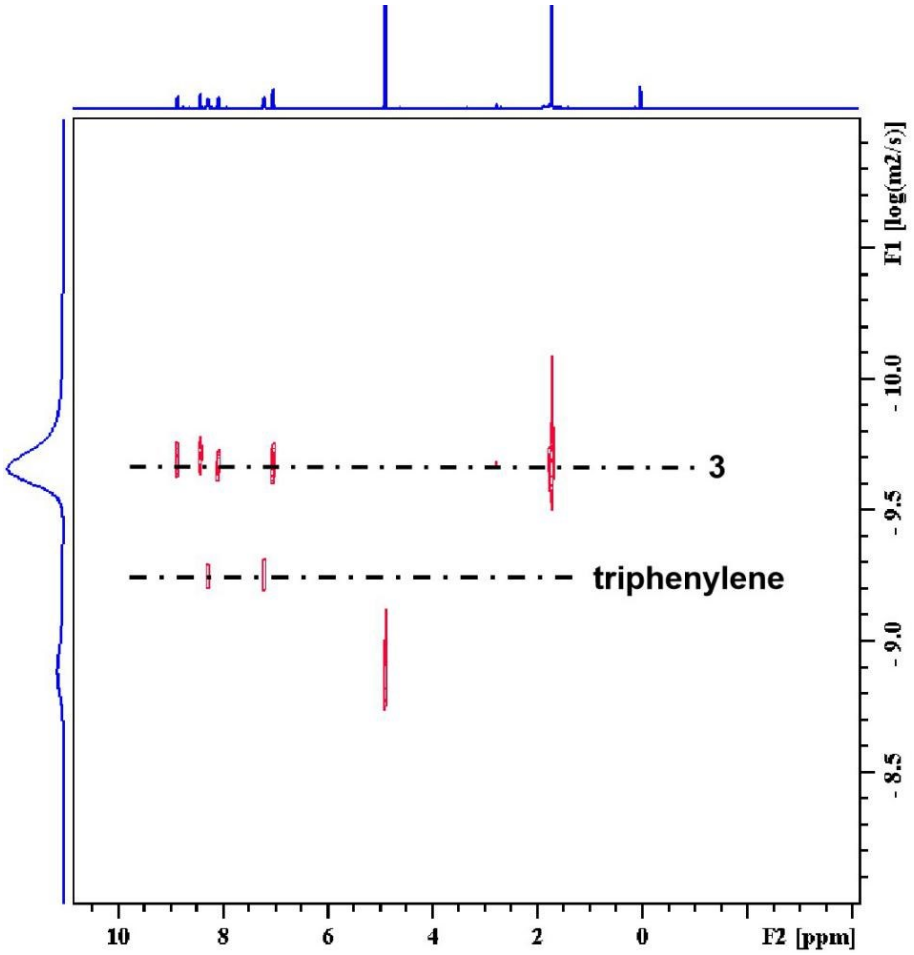

Figure S48. The ^{1}H-^{1}H DOSY NMR spectra of triphenylene encapsulated by **3** in CD_3OD.

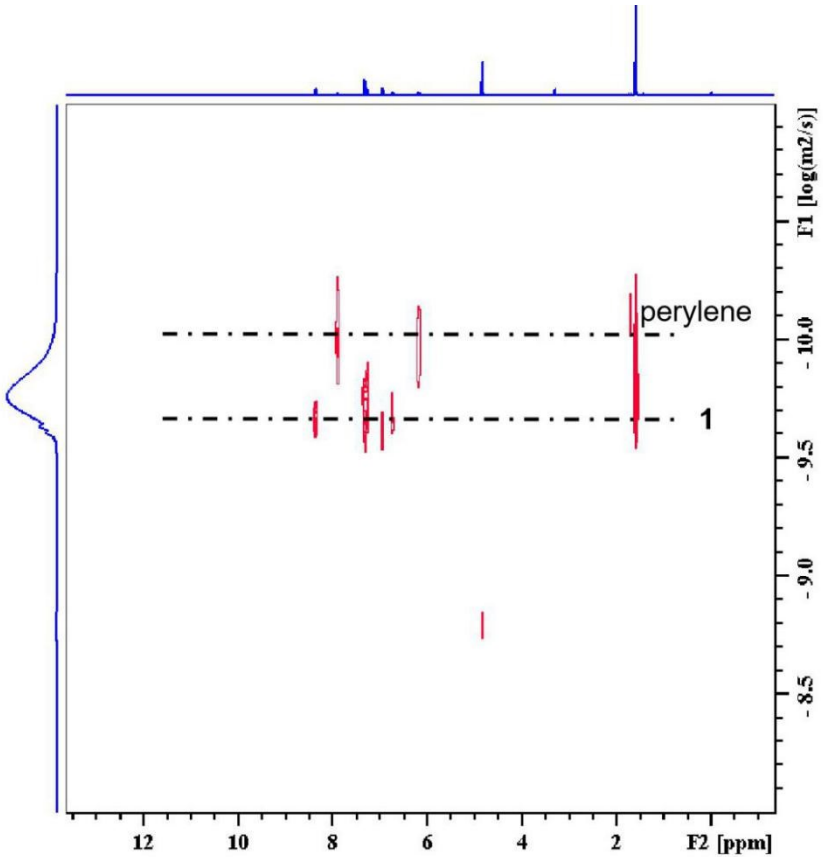

Figure S49. The ^{1}H-^{1}H DOSY NMR spectra of perylene encapsulated by **1** in CD_3OD.

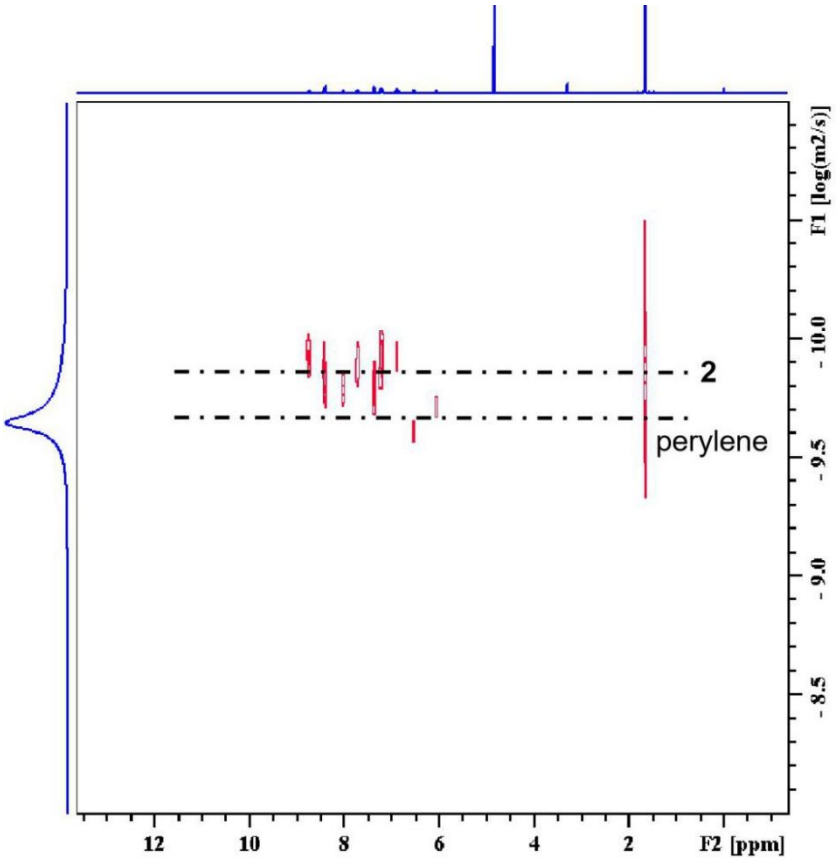

Figure S50. The ^{1}H-^{1}H DOSY NMR spectra of perylene encapsulated by **2** in CD_3OD.

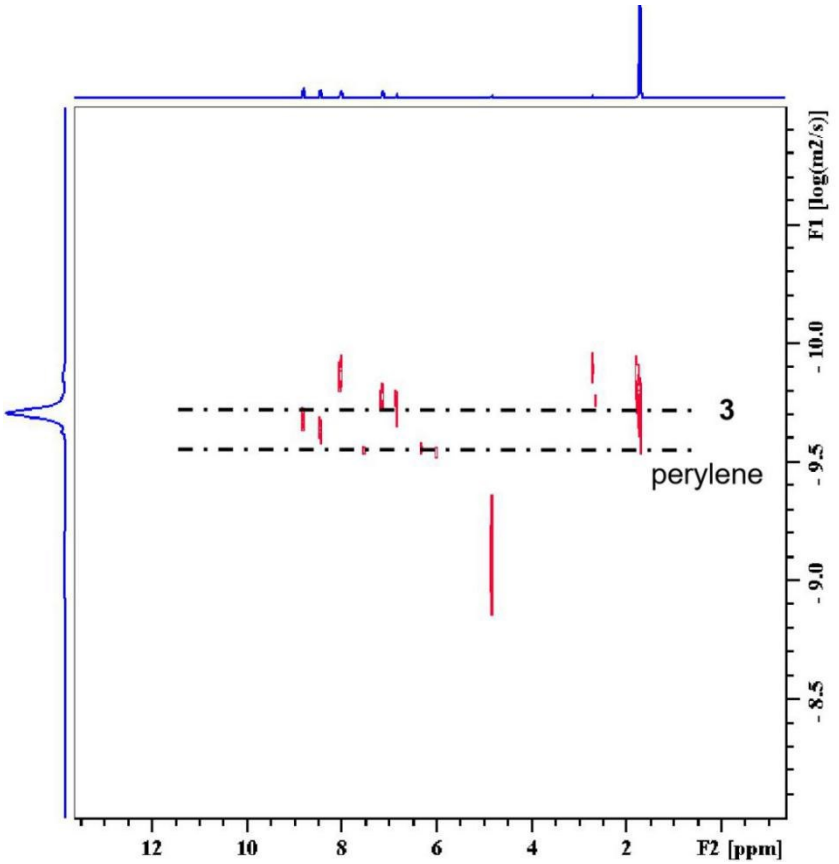

Figure S51. The ^{1}H-^{1}H DOSY NMR spectra of perylene encapsulated by **3** in CD_3OD.

2.6. Calculated binding constants *K* values based on ^{1}H NMR titrations

2.6.1 Determination of stoichiometry

Before any determination of *K* is performed, it is essential always to determine the stoichiometry of the host-guest complex. This is most readily achieved from NMR data by means of the method of continuous variations (Job's method).[4] The method of continuous variations involves preparing a series of solutions containing both the host and the guest in varying proportions so that a complete range of mole ratios is sampled ($0>[H]_0/([H]_0+[G]_0)<1$), and where the total concentration $[H]_0+[G]_0$ is constant for each solution. The experimentally observed parameter is a host or guest chemical shift that is sensitive to complex formation. The data are plotted in the form $([H]/[H]+[G])\ \Delta_{\delta H}$ versus [H]/[H]+[G]. The **Figure S50-S55** show the typical Job plots for the complexations of **1-3** and anthracene or perylene molecule. The maximum occurs at [H]/[H]+[G] = 0.5, indicating that the complex has a 1/1 (perylene molecule to **1-3**) stoichiometry.

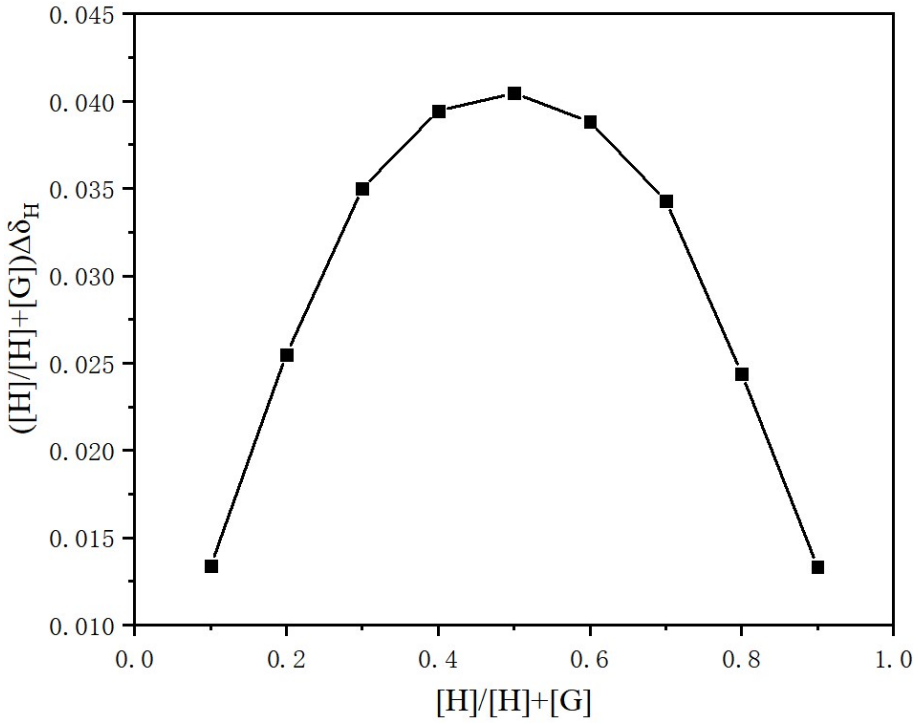

Figure S52. Illustration of the Job's plot for determination of stoichiometry (anthracene □ **1'**).

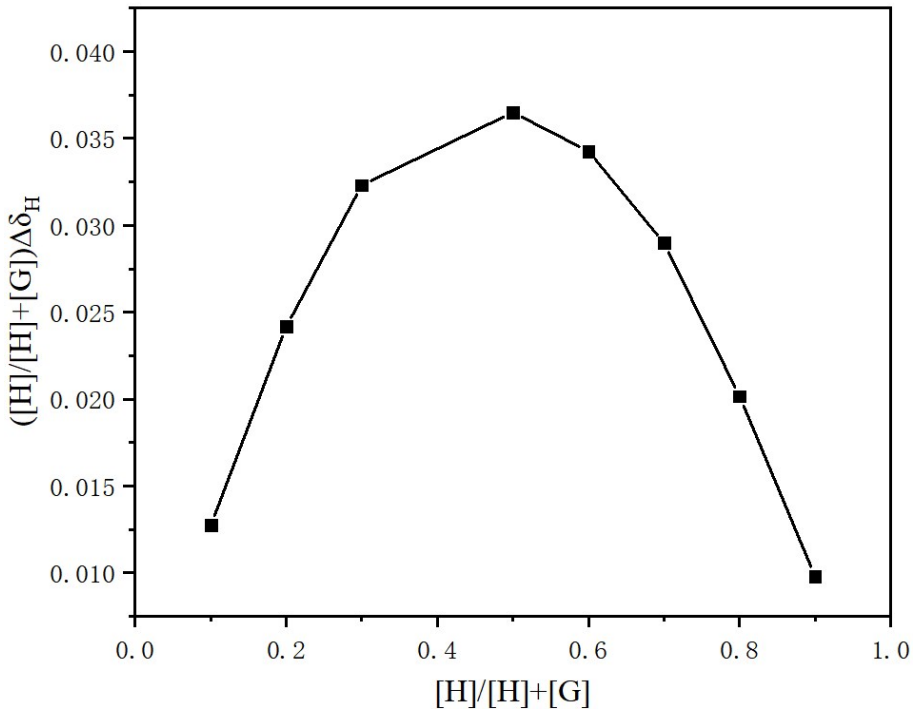

Figure S53. Illustration of the Job's plot for determination of stoichiometry (anthracene □ **2'**).

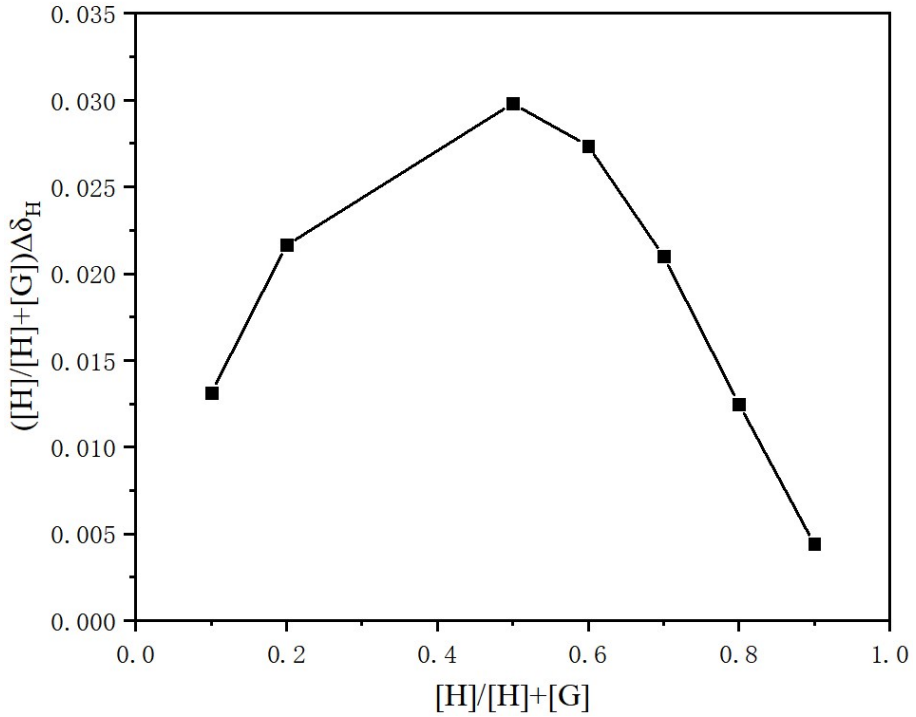

Figure S54. Illustration of the Job's plot for determination of stoichiometry (anthracene □ **3**).

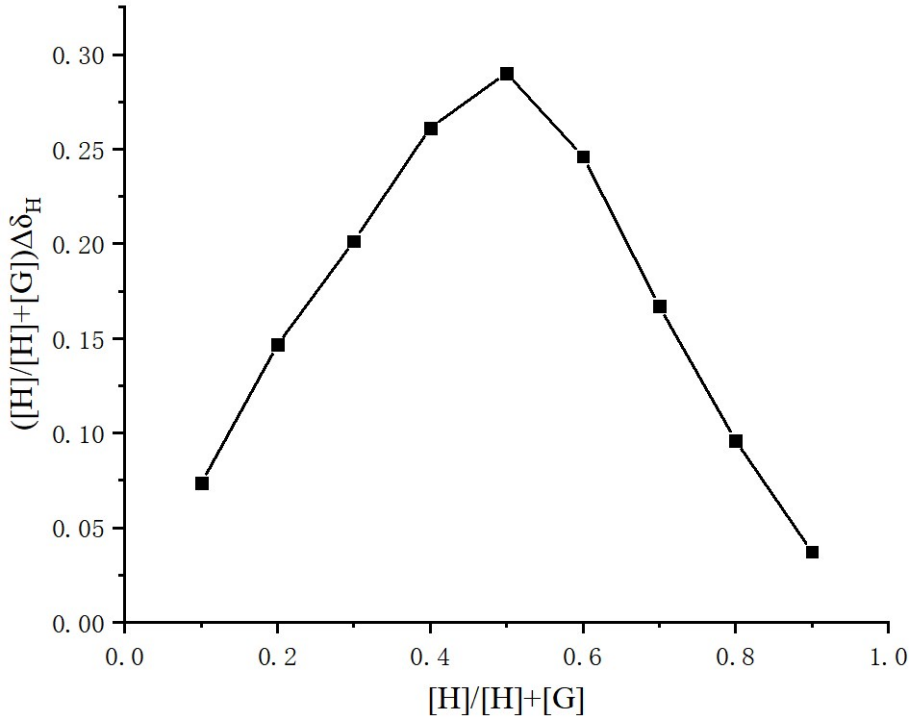

Figure S55. Illustration of the Job's plot for determination of stoichiometry (perylene□**1'**).

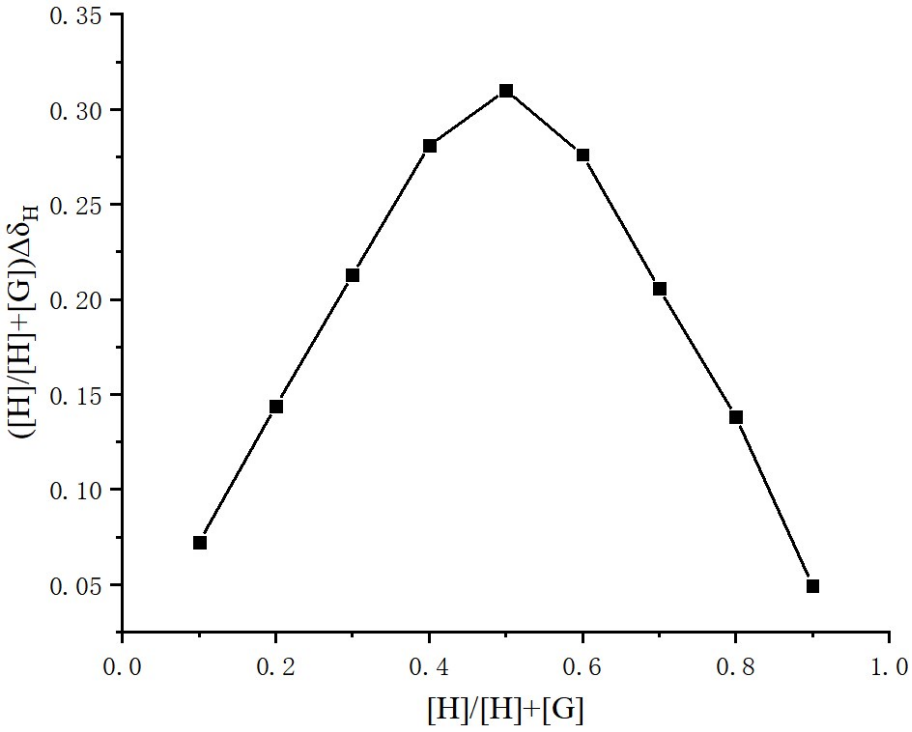

Figure S56. Illustration of the Job's plot for determination of stoichiometry (perylene□**2'**).

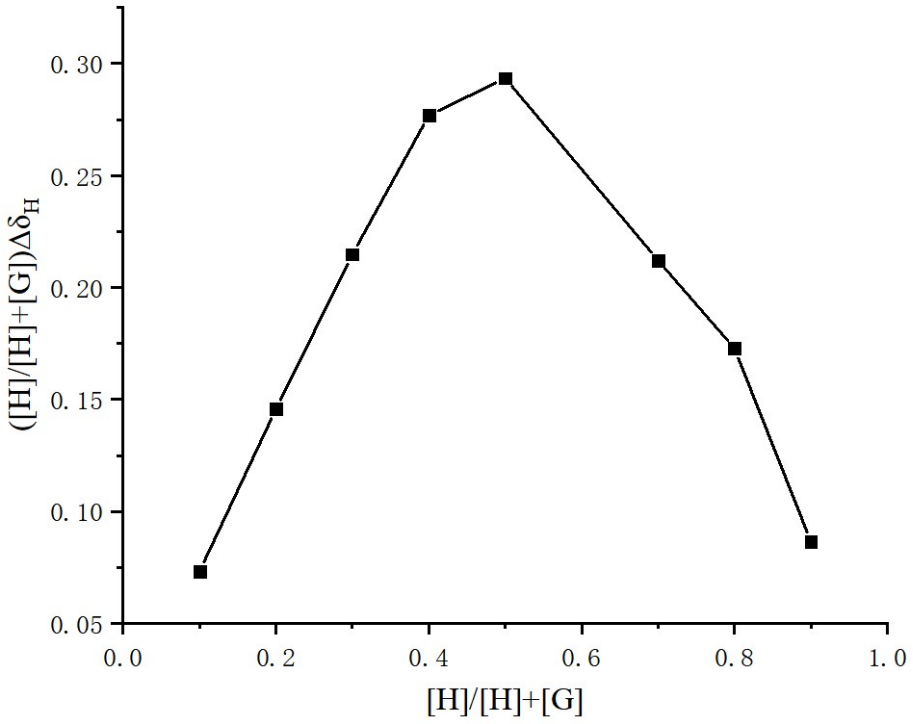

Figure S57. Illustration of the Job's plot for determination of stoichiometry (perylene□**3**).

2.6.2 Determination of Binding Constant

Procedures for NMR titrations: A 0.5 mL solution of host in CD_3OD was titrated with a concentrated solution of guests that were soluble in $CDCl_3$. The total change in concentration of the host was 5-7.9 % over the course of the titration, and the error involved was assumed to be negligible. Upon each addition, the solution was manually shaken for 10 min before acquiring the spectrum, which allowed equilibrium to be reached between the host and guest (**Figure S56-S67**).

The covariance of the fit (variance of the residuals divided by the variance in the data), along with a visual inspection of the residuals from the fit, was used to conclude that a 1:1 non-cooperative model best described the binding of guest molecules to **1-3**, which giving binding constants *K* as Table **S1**.

Table S1. The binding constants *K* of the guest molecules to complexes **1-3**.

Complexes	*K* values (M^{-1})	R^2	Standard Error
Anthracene to **1**	343.3	0.9984	28.5
Pyrene to **1**	759.2	0.9997	24.3
Triphenylene to **1**	4253.6	0.9990	280.4
Perylene to **1**	23627.8	0.9996	1919.2
Anthracene to **2**	436.3	0.9997	14.0
Pyrene to **2**	800.6	0.9998	19.1
Triphenylene to **2**	7096.6	0.9999	59.1
Perylene to **2**	13519.4	0.9952	2901.2
Anthracene to **3**	342.6	0.9998	8.5
Pyrene to **3**	1220.9	0.9965	101.6
Triphenylene to **3**	13559.6	0.9983	1240.4
Perylene to **3**	19819.7	0.9998	738.7

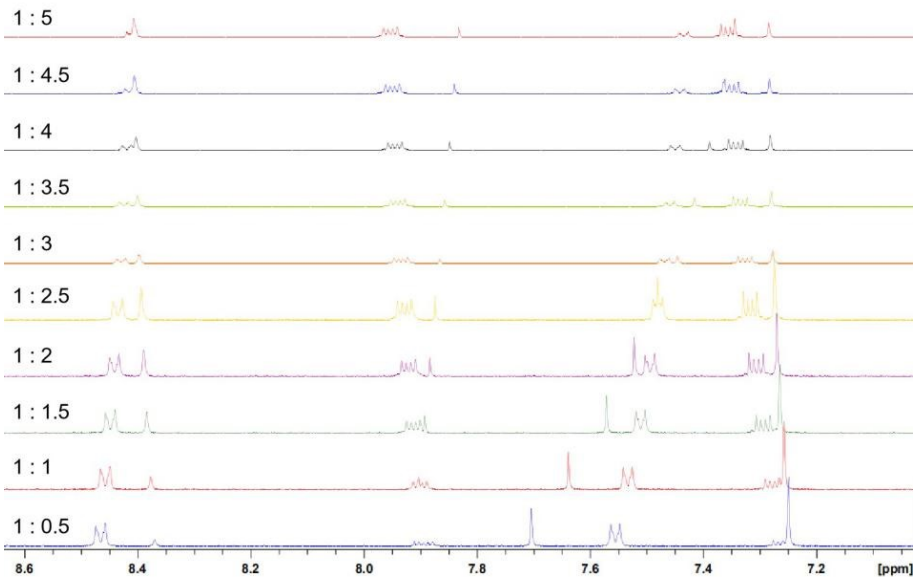

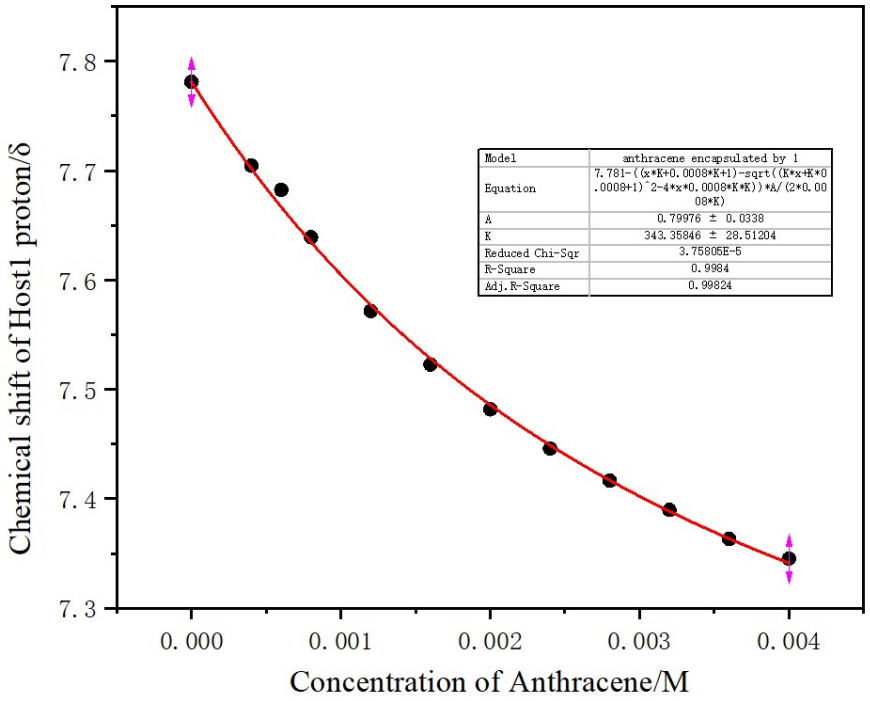

Figure S58. The NMR titration of anthracene encapsulated by **1** in CD_3OD and binding isotherms (non-cooperative 1:1 system) fitted to the chemical shift of the proton signals vs. the equivalents of anthracene added to determine the binding affinity.

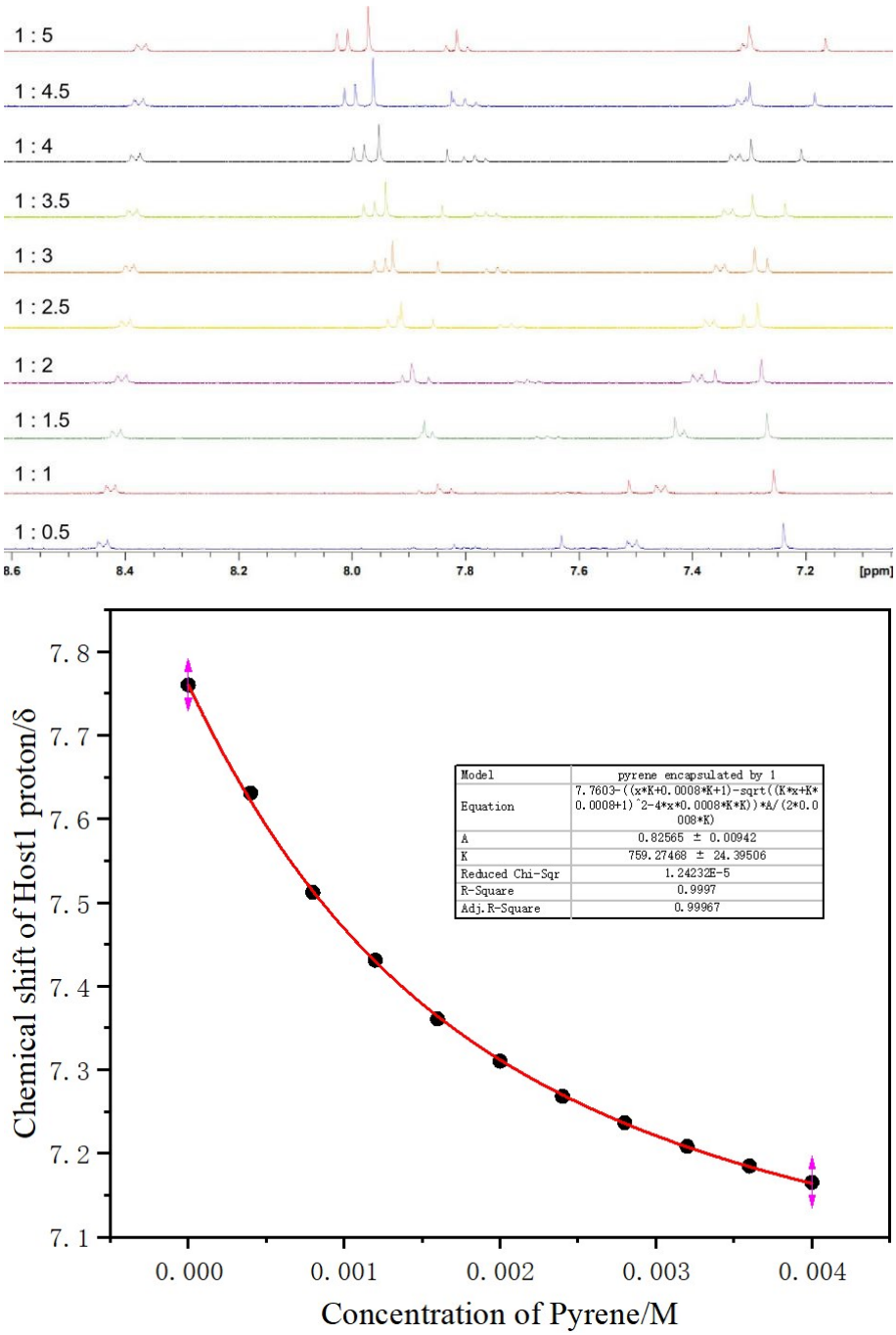

Figure S59. The NMR titration of pyrene encapsulated by **1** in CD_3OD and Binding isotherms (non-cooperative 1:1 system) fitted to the chemical shift of the proton signals vs. the equivalents of anthracene added to determine the binding affinity.

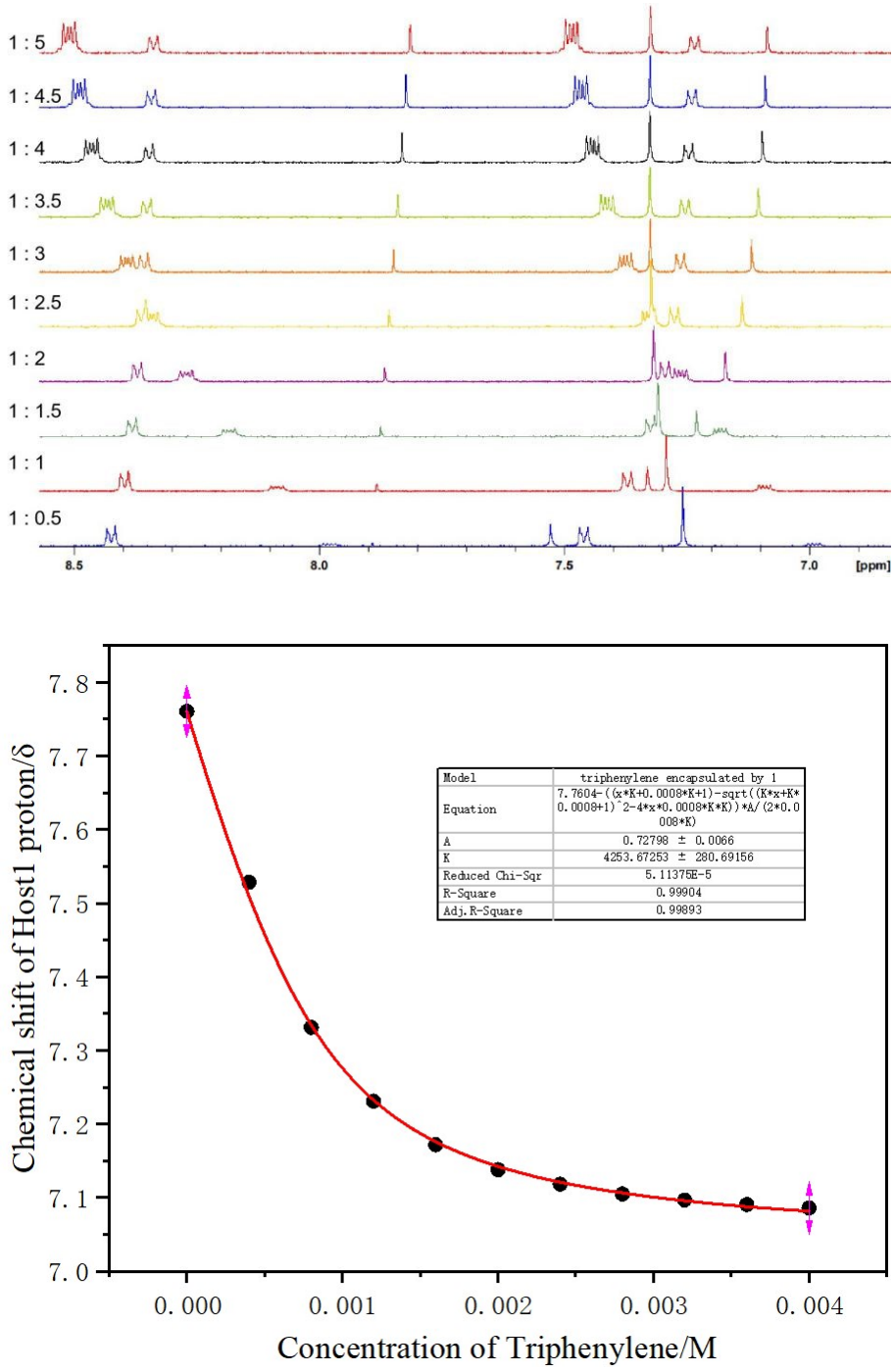

Figure S60. The NMR titration of triphenylene encapsulated by **1** in CD_3OD and Binding isotherms (non-cooperative 1:1 system) fitted to the chemical shift of the proton signals vs. the equivalents of anthracene added to determine the binding affinity.

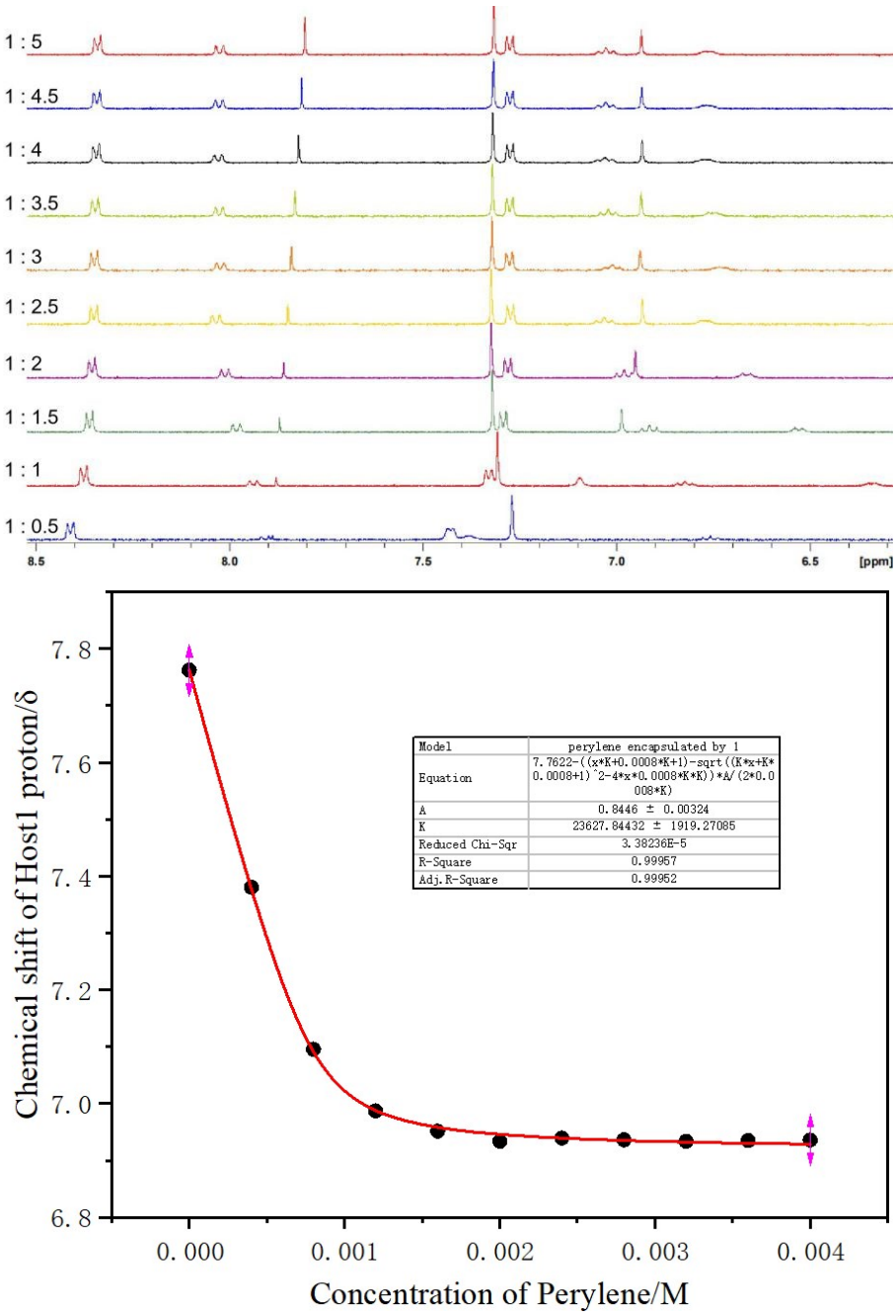

Figure S61. The NMR titration of perylene encapsulated by **1** in CD_3OD and Binding isotherms (non-cooperative 1:1 system) fitted to the chemical shift of the proton signals vs. the equivalents of anthracene added to determine the binding affinity.

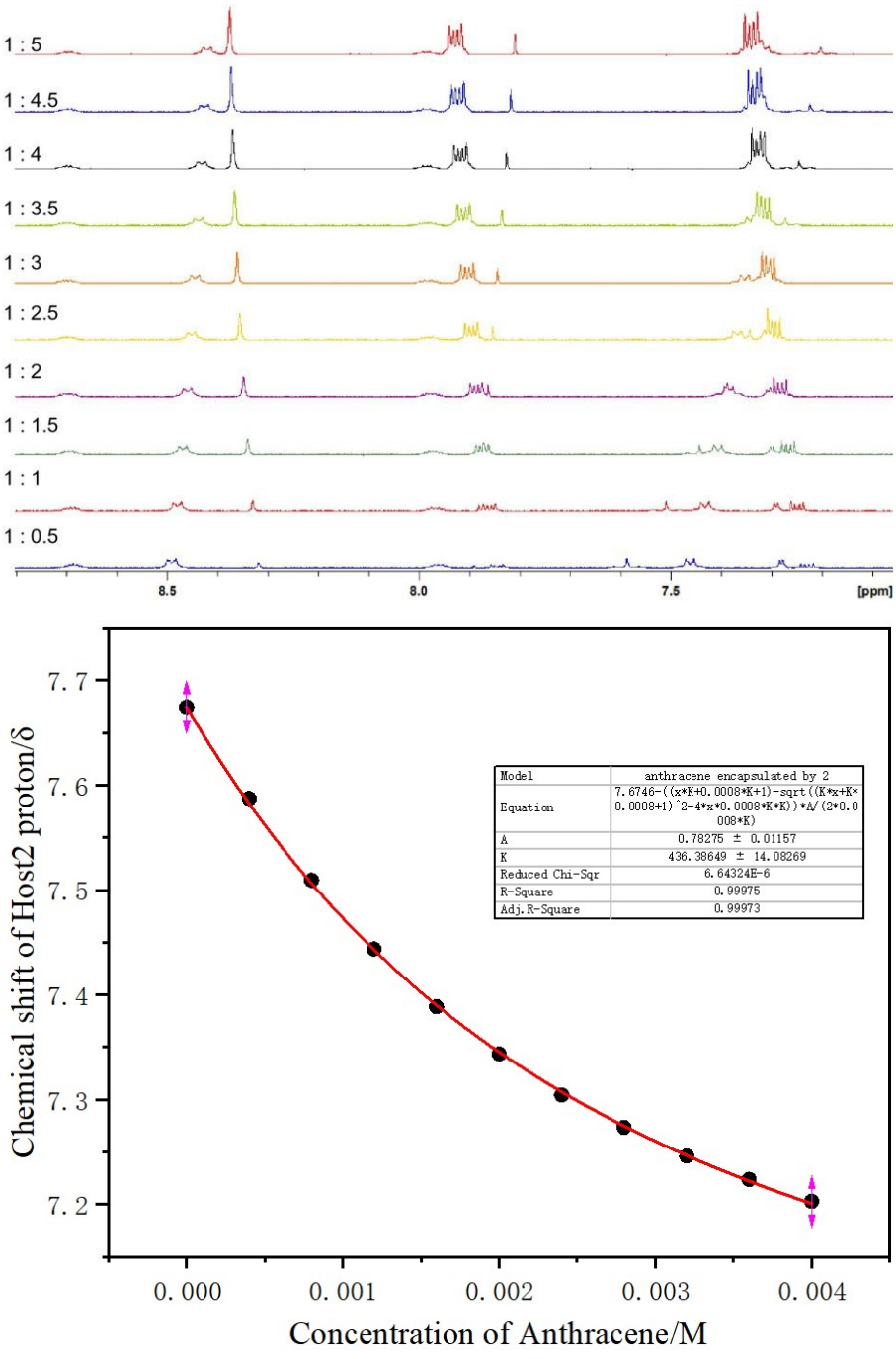

Figure S62. The NMR titration of anthracene encapsulated by **2** in CD_3OD and Binding isotherms (non-cooperative 1:1 system) fitted to the chemical shift of the proton signals vs. the equivalents of anthracene added to determine the binding affinity.

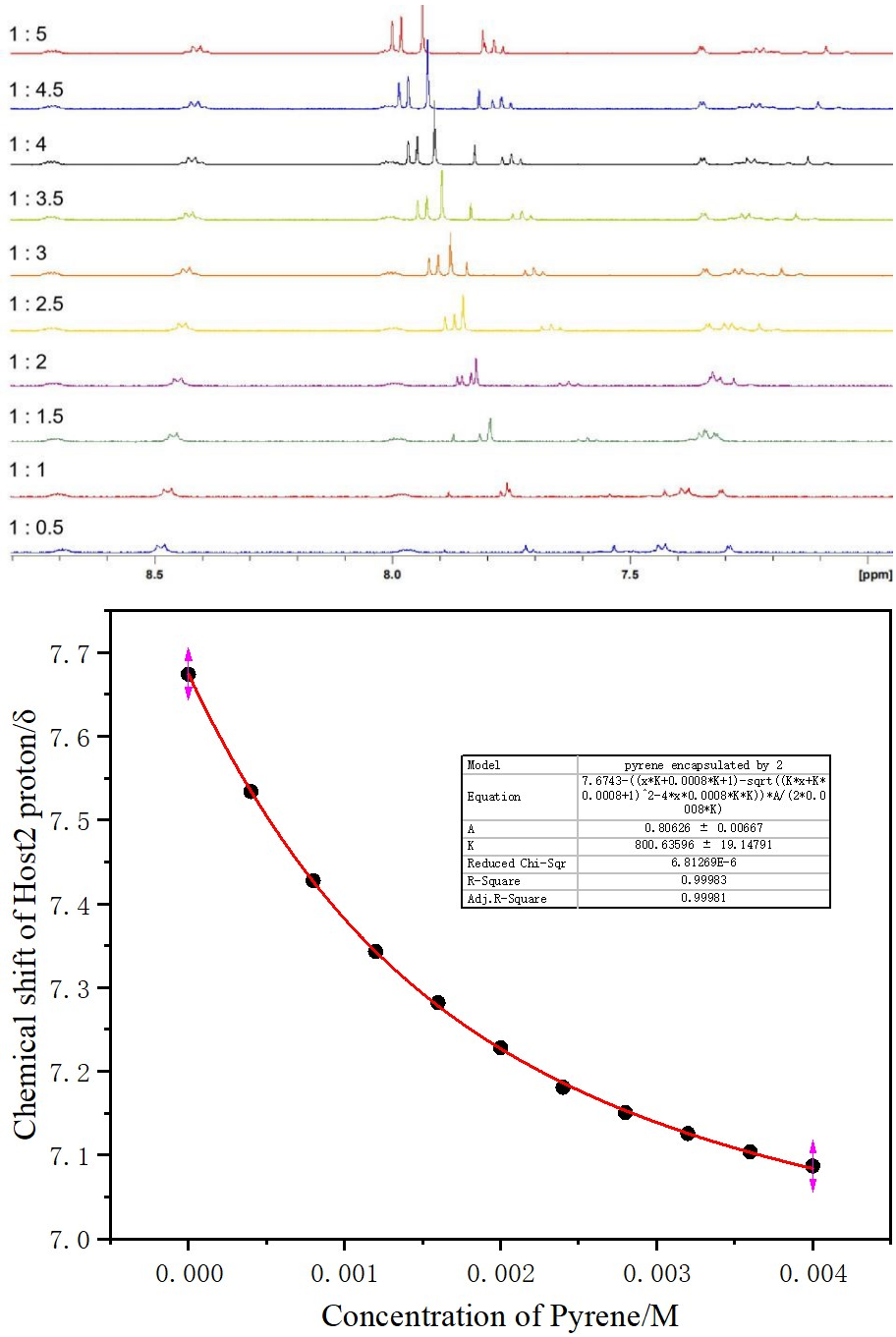

Figure S63. The NMR titration of pyrene encapsulated by **2** in CD_3OD and Binding isotherms (non-cooperative 1:1 system) fitted to the chemical shift of the proton signals vs. the equivalents of anthracene added to determine the binding affinity.

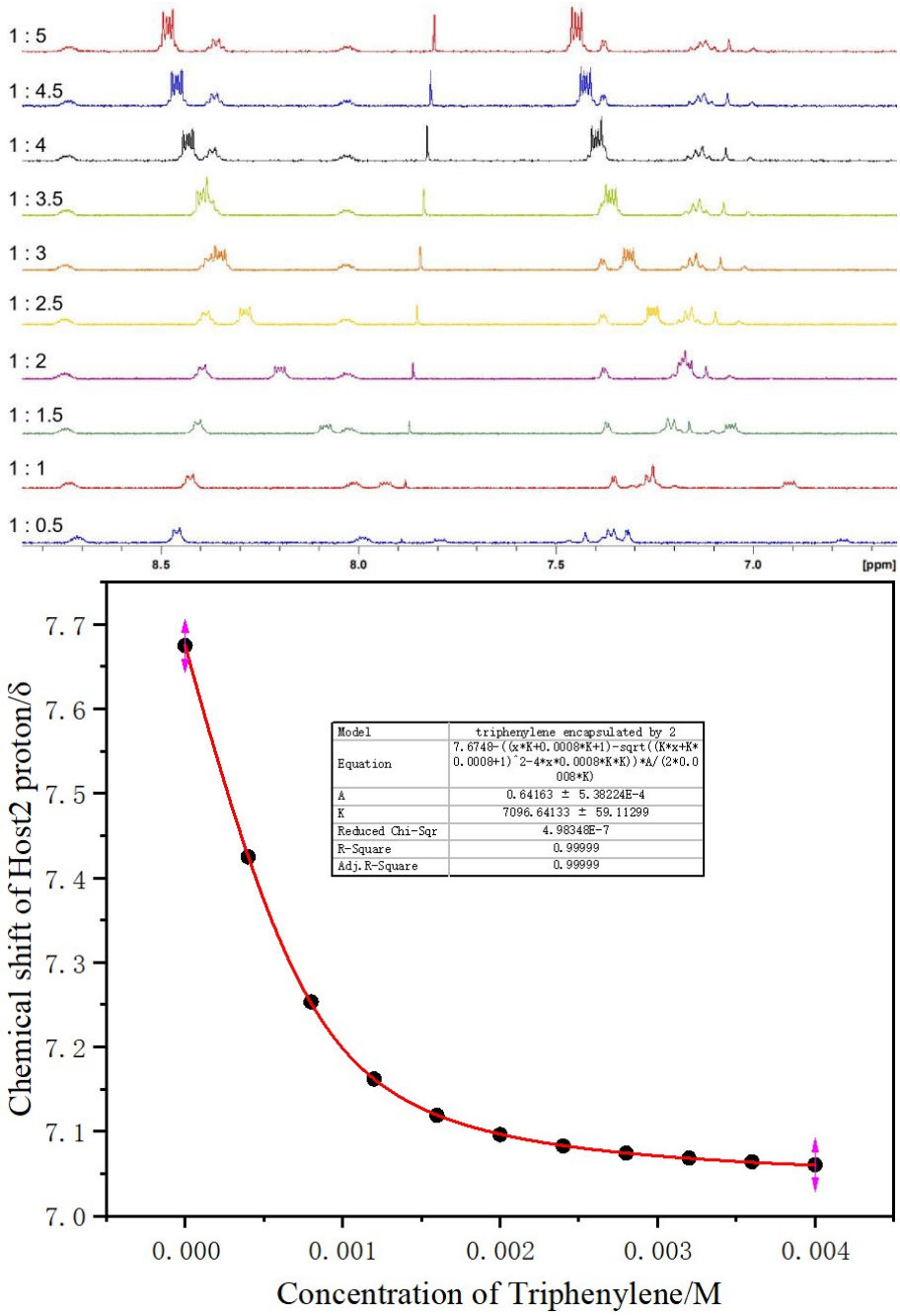

Figure S64. The NMR titration of triphenylene encapsulated by **2** in CD_3OD and Binding isotherms (non-cooperative 1:1 system) fitted to the chemical shift of the proton signals vs. the equivalents of anthracene added to determine the binding affinity.

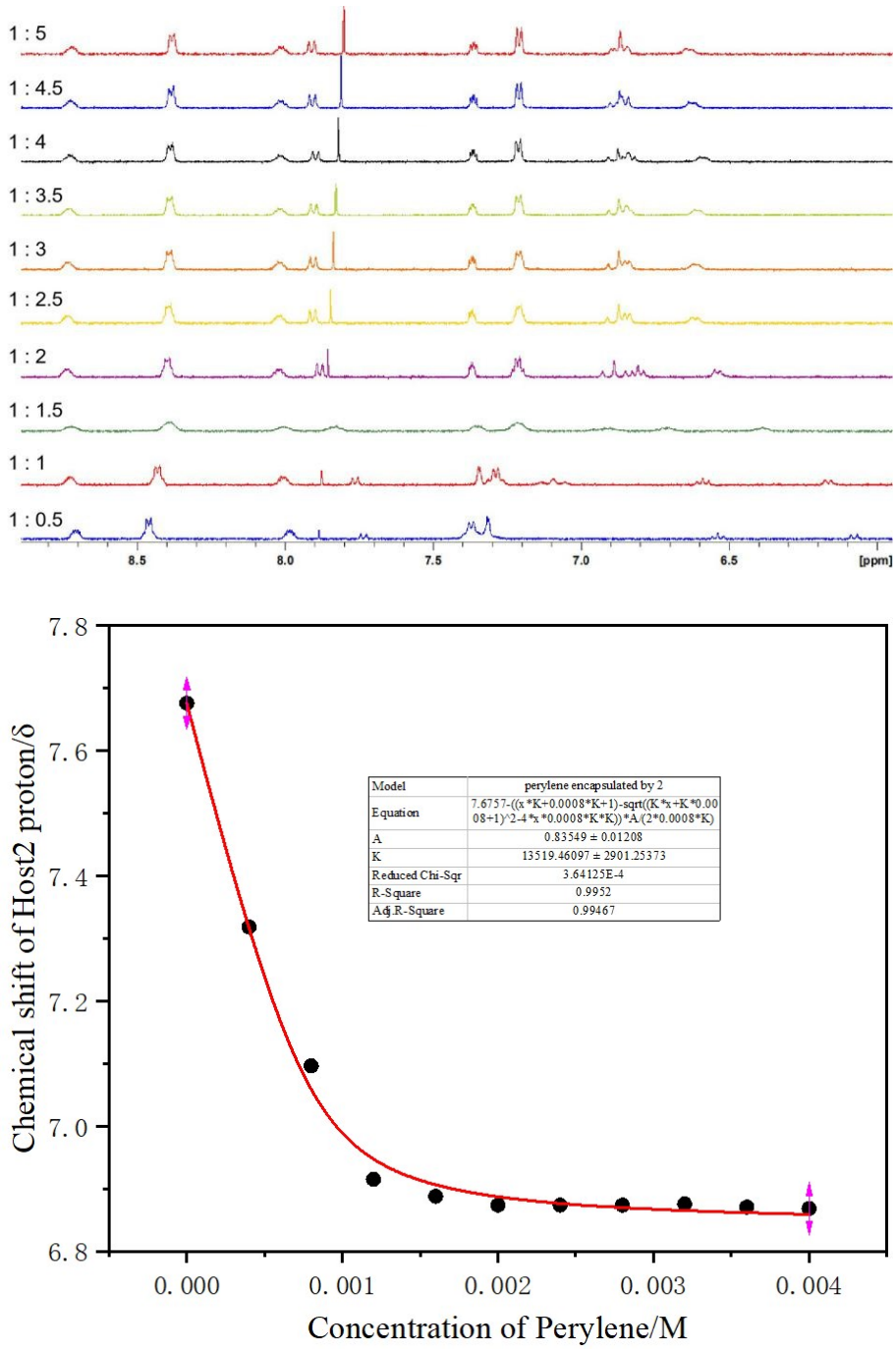

Figure S65. The NMR titration of perylene encapsulated by **2** in CD_3OD and Binding isotherms (non-cooperative 1:1 system) fitted to the chemical shift of the proton signals vs. the equivalents of anthracene added to determine the binding affinity.

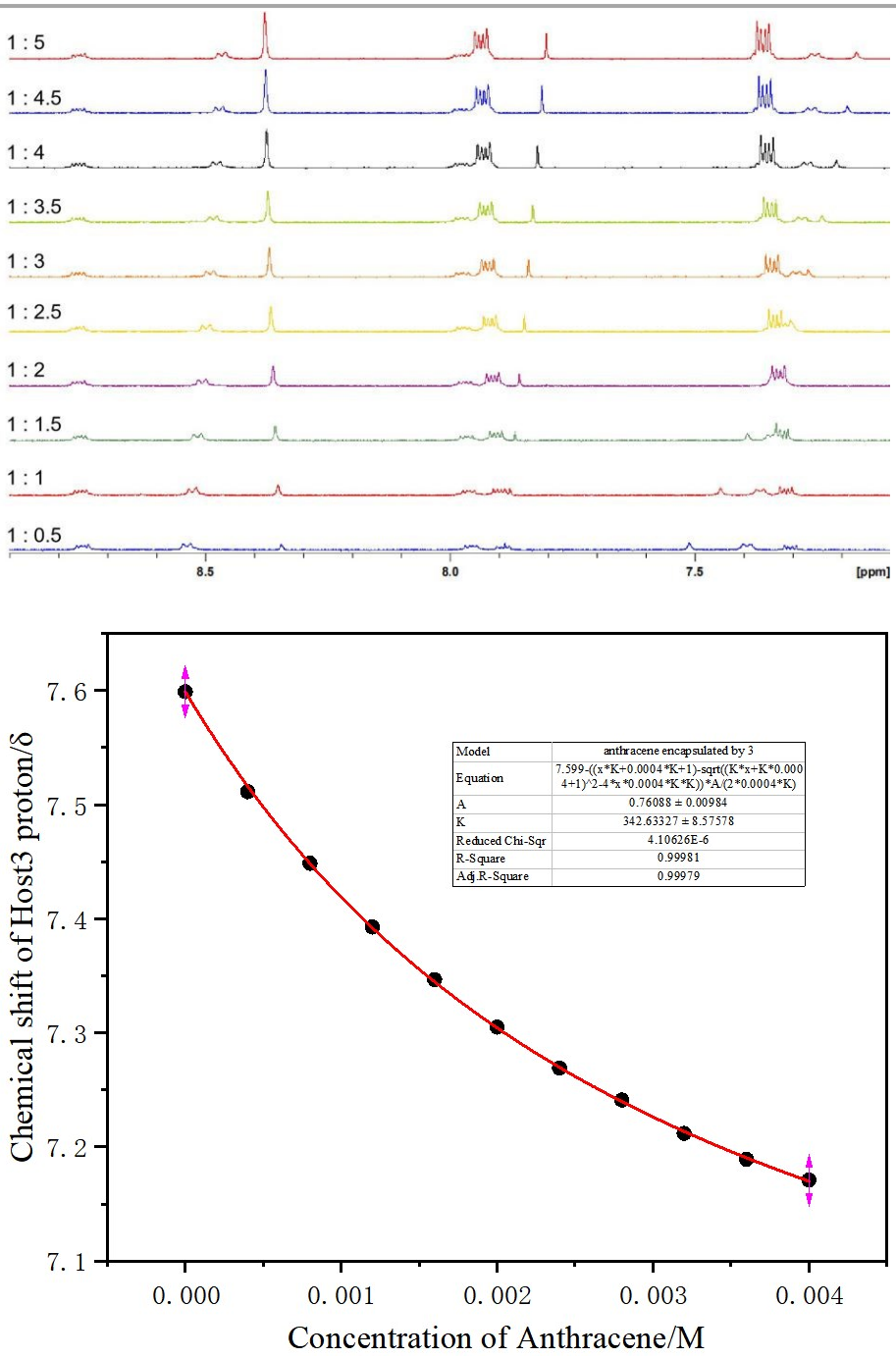

Figure S66. The NMR titration of anthracene encapsulated by **3** in CD_3OD and Binding isotherms (non-cooperative 1:1 system) fitted to the chemical shift of the proton signals vs. the equivalents of anthracene added to determine the binding affinity.

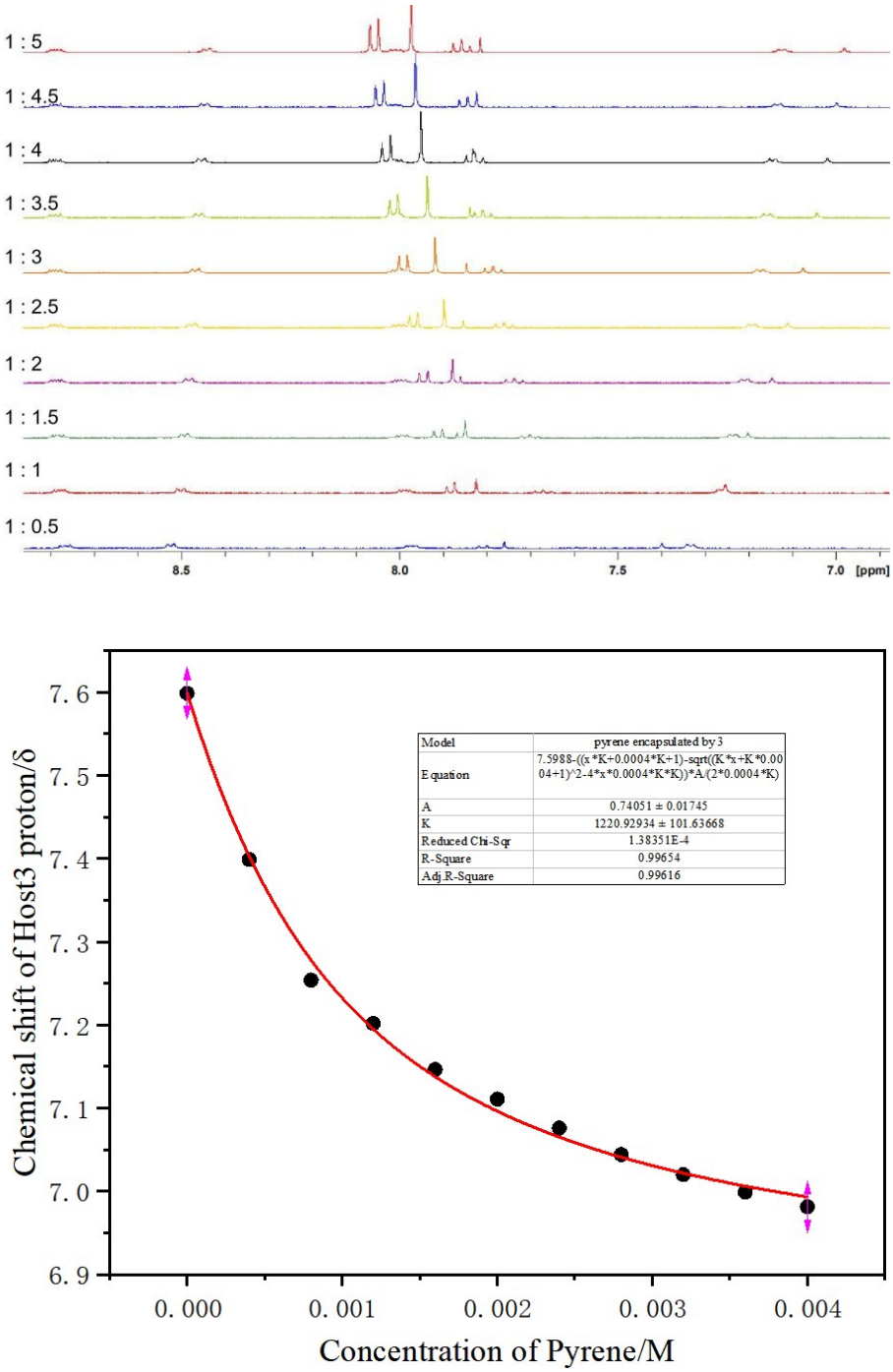

Figure S67. The NMR titration of pyrene encapsulated by **3** in CD_3OD and Binding isotherms (non-cooperative 1:1 system) fitted to the chemical shift of the proton signals vs. the equivalents of anthracene added to determine the binding affinity.

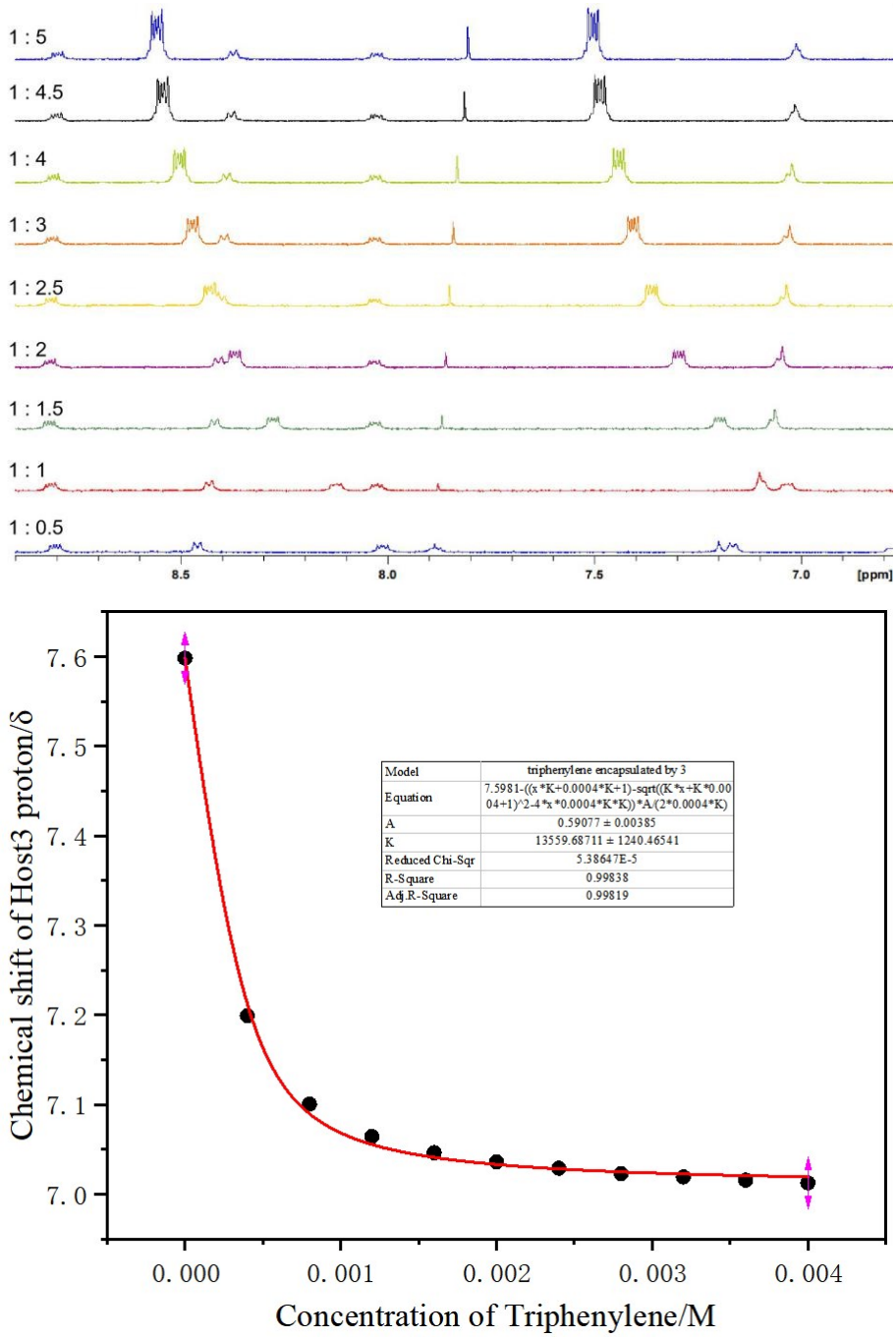

Figure S68. The NMR titration of triphenylene encapsulated by **3** in CD_3OD and Binding isotherms (non-cooperative 1:1 system) fitted to the chemical shift of the proton signals vs. the equivalents of anthracene added to determine the binding affinity.

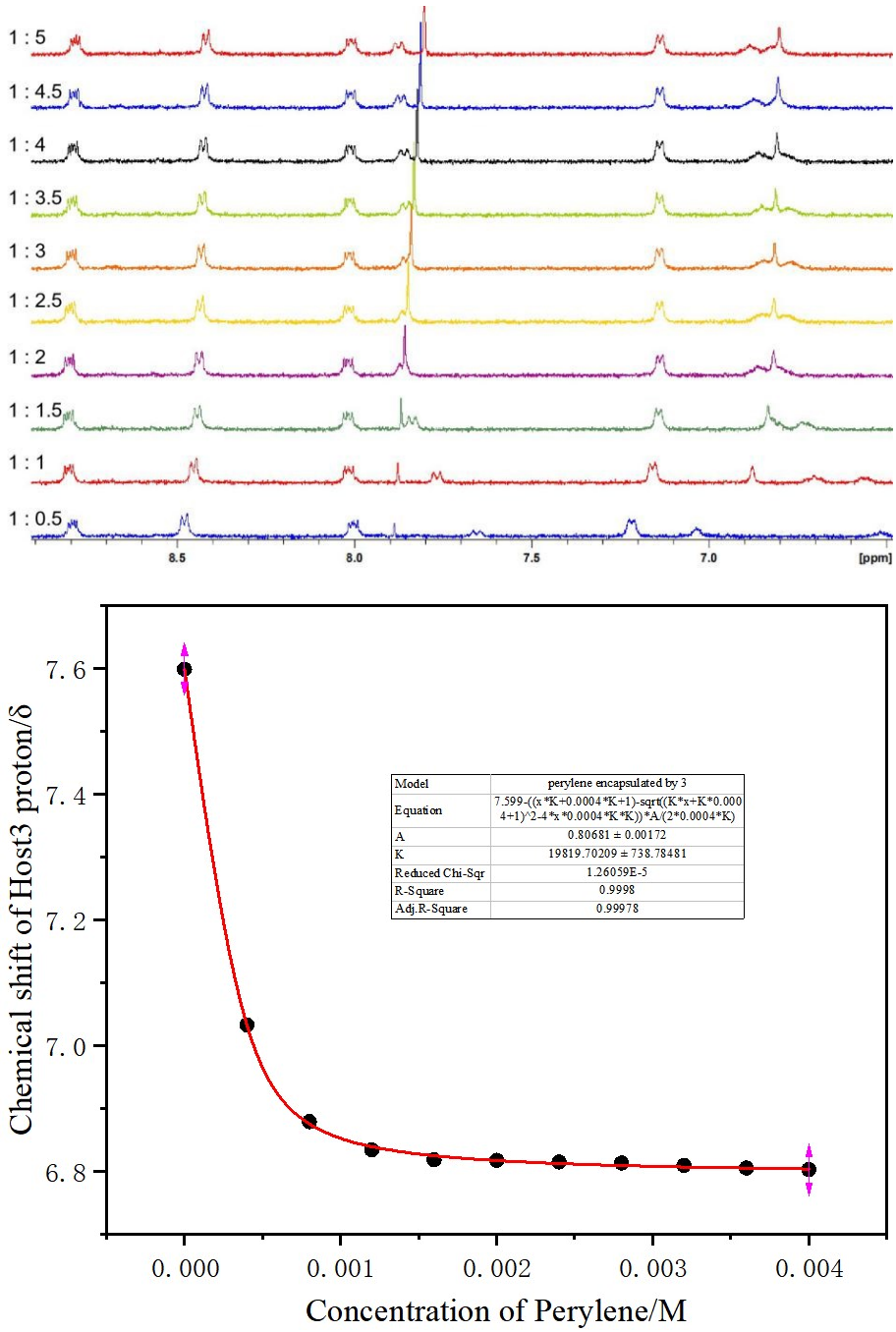

Figure S69. The NMR titration of perylene encapsulated by **3** in CD_3OD and Binding isotherms (non-cooperative 1:1 system) fitted to the chemical shift of the proton signals vs. the equivalents of anthracene added to determine the binding affinity.

2.7 IR spectra of complexes 1-3

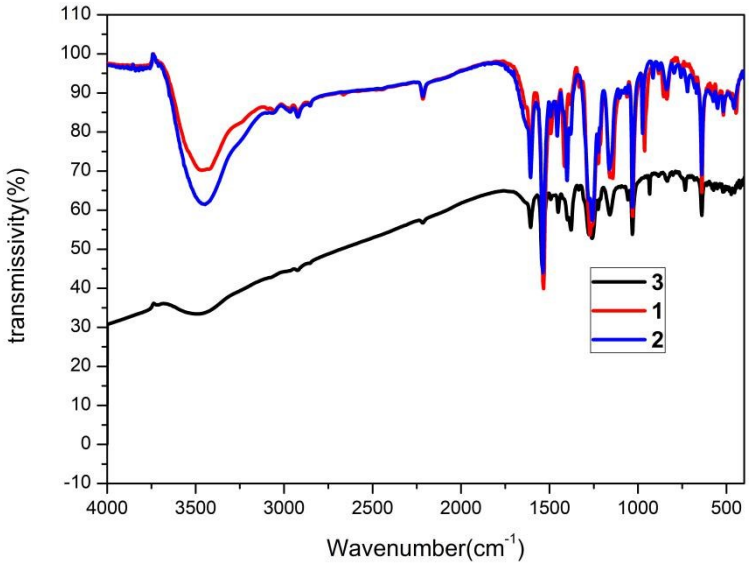

Figure S70. IR spectra of complexes **1-3**.

2.8 TGA curves of complexes 1 and 2

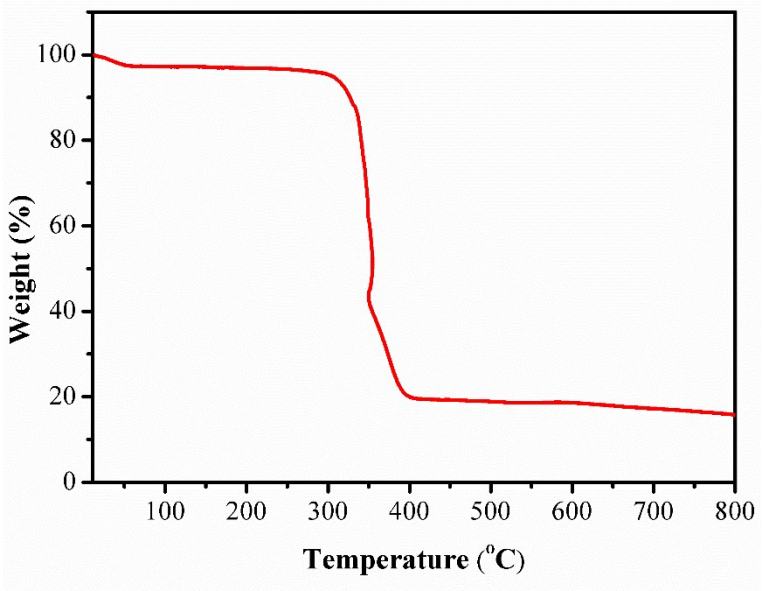

Figure S71. TGA curve of complex **1**.

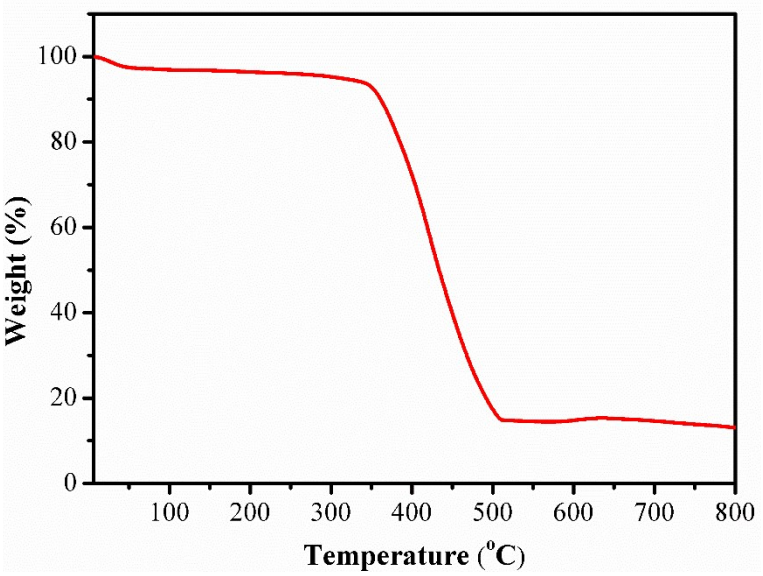

Figure S72. TGA curve of complex **2**.

3. Crystal data of 1 and 2

Table S2. Crystal data of **1** and **2**.

	1	**2**
Formula	$C_{178}H_{190}F_{18}N_{12}O_{34}Rh_6S_6$	$C_{172}H_{200}F_{18}N_6O_{51}Rh_6S_6$
M_r	4193.23	4319.19
T [K]	173	173
Crystal system	triclinic	monoclinic
Space group	P-1	$P2_1/n$
a [Å]	17.6122(10)	35.2854(19)
b [Å]	22.2298(14)	32.1734(18)
c [Å]	26.3632(14)	37.719(2)
α [°]	70.629(4)	90
β [°]	81.477(3)	101.939(3)
γ [°]	72.911(4)	90
V [Å^3]	9292.7(10)	41894(4)
Z	2	8
ρ_{calcd} [g cm^{-3}]	1.499	1.370
F(000)	4284	17680
Crystal size [mm^3]	0.360 × 0.310 × 0.280	0.124 × 0.058 × 0.057
$2\theta_{max}$ [°]	74.916	41.826
Reflections collected	243712	275446
Independent reflections	37934	42711
Parameters	1822	2887
R_1 [$I > 2\sigma(I)$]	0.0690	0.1843
wR_2 [all data]	0.2283	0.4126
GooF	1.080	1.122
CCDC number	2021986	2021987

4. References

1 C. White, A.Yates, P. M. Maitlis and D. M. Heinekey, *Inorg. Synth.,* 1992, **29**, 228-234.

2 a) G. M. Sheldrick, *Acta Cryst.*, 2015, **A71**, 3-8; b) G. M. Sheldrick, *Acta Cryst.*, 2015, **C71**, 3-8.

3 O. V. Dolomanov, L. J. Bourhis, R. J. Gildea, J. A. K. Howard and H. Puschmann, *J. Appl. Cryst.*, 2009, **42**, 339-341.

4 L. Fielding, *Tetrahedron,* 2000, **56**, 6151-6170.